Molecular Medicine 4: 299-323, 1998

Molecular Medicine

Original Articles

Convergence and Divergence of the Signaling Pathways for Insulin and Phosphoinositolglycans

Günter Müller, Susanne Wied, Christine Piossek, Andrea Bauer, Jochen Bauer, and Wendelin Frick
Hoechst Marion Roussel Deutschland GmbH, Frankfurt am Main, Germany

Communicated by P. Cuatrecasas. Accepted March 1, 1998

Abstract

Phosphoinositolglycan molecules isolated from insulin-sensitive mammalian tissues have been demonstrated in numerous in vitro studies to exert partial insulin-mimetic activity on glucose and lipid metabolism in insulin-sensitive cells. However, their ill-defined structures, heterogeneous nature, and limited availability have prohibited the analysis of the underlying molecular mechanism. Phosphoinositolglycan-peptide (PIG-P) of defined and homogeneous structure prepared in large scale from the core glycan of a glycosyl-phosphatidylinositol-anchored membrane protein from *Saccharomyces cerevisiae* has recently been shown to stimulate glucose transport as well as a number of glucose-metabolizing enzymes and pathways to up to 90% (at 2 to 10 μm) of the maximal insulin effect in isolated rat adipocytes, cardiomyocytes, and diaphragms (G. Müller et al., 1997, *Endocrinology* **138:** 3459–3476). Consequently, we used this PIG-P for the present study in which we compare its intracellular signaling with that of insulin. The activation of glucose transport by both PIG-P and insulin in isolated rat adipocytes and diaphragms was found to require stimulation of phosphatidylinositol (PI) 3-kinase but to be independent of functional p70S6kinase and mitogen-activated protein kinase. The increase in glycerol-3-phosphate acyltransferase activity in rat adipocytes in response to PIG-P and insulin was dependent on both PI 3-kinase and p70S6kinase. This suggests that the signaling pathways for PIG-P and insulin to glucose transport and metabolism converge at the level of PI 3-kinase. A component of the PIG-P signaling pathway located upstream of PI 3-kinase was identified by desensitization of isolated rat adipocytes for PIG-P action by combined treatment with trypsin and NaCl under conditions that preserved cell viability and the insulin-mimetic activity of sodium vanadate but completely blunted the insulin response. Incubation of the cells with either trypsin or NaCl alone was ineffective. The desensitized adipocytes were reconstituted for stimulation of lipogenesis by PIG-P by addition of the concentrated trypsin/salt extract. The reconstituted adipocytes exhibited 65–75% of the maximal PIG-P response and similar EC_{50} values for PIG-P (2 to 5 μm) compared with control cells. A proteinaceous *N*-ethylmaleimide (NEM)-sensitive component contained in the trypsin/salt extract was demonstrated to bind in a functional manner to the adipocyte plasma membrane of desensitized adipocytes via bipolar interactions. An excess of trypsin/salt extract inhibited PIG-P action in untreated adipocytes in a competitive fashion compatible with a receptor function for PIG-P of this protein. The presence of the putative PIG-P receptor protein in detergent-insoluble complexes prepared from isolated rat adipocytes suggests that caveolae/detergent–insoluble complexes of the plasma membrane may play a role in insulin-mimetic signaling by PIG-P. Furthermore, treatment of isolated rat diaphragms and adipocytes with PIG-P as well as with other agents exerting partially insulin-mimetic activity, such as PI-specific phospholipase C (PLC) and the sulfonylurea glimepiride, triggered tyrosine phosphorylation of the caveolar marker protein caveolin, which was apparently correlated with stimulation of lipogenesis. Strikingly, in adipocytes subjected to combined trypsin/salt treatment, PIG-P, PI-specific PLC, and glimepiride failed completely to provoke insulin-mimetic effects. A working model is presented for a signaling pathway in insulin-sensitive cells used by PIG(-P) molecules which involves GPI structures, the trypsin/salt– and NEM-sensitive receptor protein for PIG-P, and additional proteins located in caveolae/detergent–insoluble complexes.

Introduction

Two pathways within the insulin-signaling network have been dissected and are thought to mediate different biological functions of the hormone (for reviews see refs. 1–4). The first is activation of phosphatidylinositol 3 (PI 3)-kinase, which plays a pivotal role in stimulation of glucose transport by insulin and in the regulation of cellular trafficking (5,6; for a review see ref. 7). The second pathway is formation of the Shc-Grb2 complex, which leads to activation of the Ras/mitogen-activated protein kinase (MAPK) pathway. This latter pathway has been linked to insulin regulation of both cell growth and gene expression (8; for a review see ref. 9), although this linkage has been questioned recently. Many studies in vitro have demonstrated that insulin signaling and consequently, these two basic pathways can be modulated in a positive and negative fashion by a variety of factors (for reviews see refs. 1,10,11), including proteins (e.g., angiotensin II, growth hormone, leptin, PC-1, Rad, tumor necrosis factor-alpha [TNF-α]) and small molecules (e.g., catecholamines). Soluble phosphoinositolglycan (PIG) molecules that have been shown to exert partial insulin-mimetic effects in diverse cellular and subcellular systems (for reviews see refs. 12, 13) can also be classified in the latter category.

Initially, this material was thought to be of a peptidic nature (for a review see ref. 14). However, subsequent analysis revealed that it can be generated from a lipidic precursor structure (15) as the polar headgroup consisting of phosphoinositolglycan (16,17), which may harbor *chiro*-inositol (18). Whereas the detailed structure of the insulin-sensitive PIG molecules with putative mediator function is still in dispute, a minimal consensus on the composition of PIG compounds (based in particular on analytic and metabolic labeling studies as well as on chemical and enzymatic modifications) has developed. They appear to consist of a core structure of phosphorylated *myo/chiro*-inositol that is glycosidically linked to nonacetylated hexosamine which in turn is coupled to an oligosaccharide of varying composition, often containing mannose and galactose residues (for reviews see refs. 12,13). Thus, PIG molecules resemble the polar core glycan head groups of both free glycosylphosphatidylinositol (GPI) lipids and GPI membrane anchors of so-called GPI-anchored proteins, which are embedded in the plasma membrane by a covalently bound glycolipid (for reviews see refs. 19–22). The PIG portion of GPI anchors consists of phosphoinositol, nonacetylated glucosamine, and an oligosaccharide that in all GPI-anchored proteins investigated so far, from yeast and parasites to humans, consists of three mannose residues linked in a characteristic glycosidic manner (Fig. 1). Unfortunately, despite extensive efforts, the detailed structure of a PIG molecule from insulin-sensitive tissues exhibiting insulin-mimetic activity has not been elucidated. Therefore, the only source of a sufficient quantity of PIG molecules of defined structure is the core glycans of GPI-anchored proteins.

We prepared PIG molecules of defined structure as phosphoinositolglycan-peptide (PIG-P) derived from the GPI-anchored protein Gce1p of the yeast *Saccharomyces cerevisiae* (23) using sequential lipolytic and proteolytic digestion (24). Interestingly, isolated rat and cultured 3T3-L1 adipocytes contain a similar GPI-anchored protein with respect to size and the ability to bind cAMP—Gce1—which is susceptible to lipolytic cleavage in response to insulin and the sulfonylurea glimepiride (25–27). So far, the pysiological relevance of activation of the relevant phospholipase C (PLC) remains unclear, but it has been implicated with metabolic signaling (see Discussion). The PIG-P from yeast Gce1p can be obtained in considerable amounts using large-scale fermentation technology. The preparation protocol includes the isolation and purification of Gce1p and sequential generation of GPI peptides by digestion with V8 protease from *Staphylococcus aureus* and of PIG peptides by treatment with PI-specific PLC from *Bacillus cereus* (see Fig. 1A, [24]), followed by purification to radiochemical and chemical homogeneity. The structure of the PIG-P is completely defined and consists of the typical PIG structure that is identical to that of mammalian and yeast GPI-anchored proteins. The PIG-P is coupled via a phosphoethanolamine bridge and an amide linkage to the tripeptide H-Tyr-Cys-Asn, derived from the carboxy terminus of Gce1p (see Fig. 1B). This molecule can be specifically degraded by chemical means, such as dephosphorylation with aqueous hydrogen fluoride or deamination of the nonacetylated glucosamine with nitrous acid, or enzymatically, using pronase (see Fig. 1A).

When assayed for insulin-mimetic activity in

Address correspondence and reprint requests to: Dr. Günter Müller, Hoechst Marion Roussel Deutschland GmbH, Metabolic Diseases Research Bldg. H825, D-65926 Frankfurt am Main, Germany. Phone: 4969-305-4271; Fax: 4969-305-81767; E-mail: guenter.mueller@hmrag.com

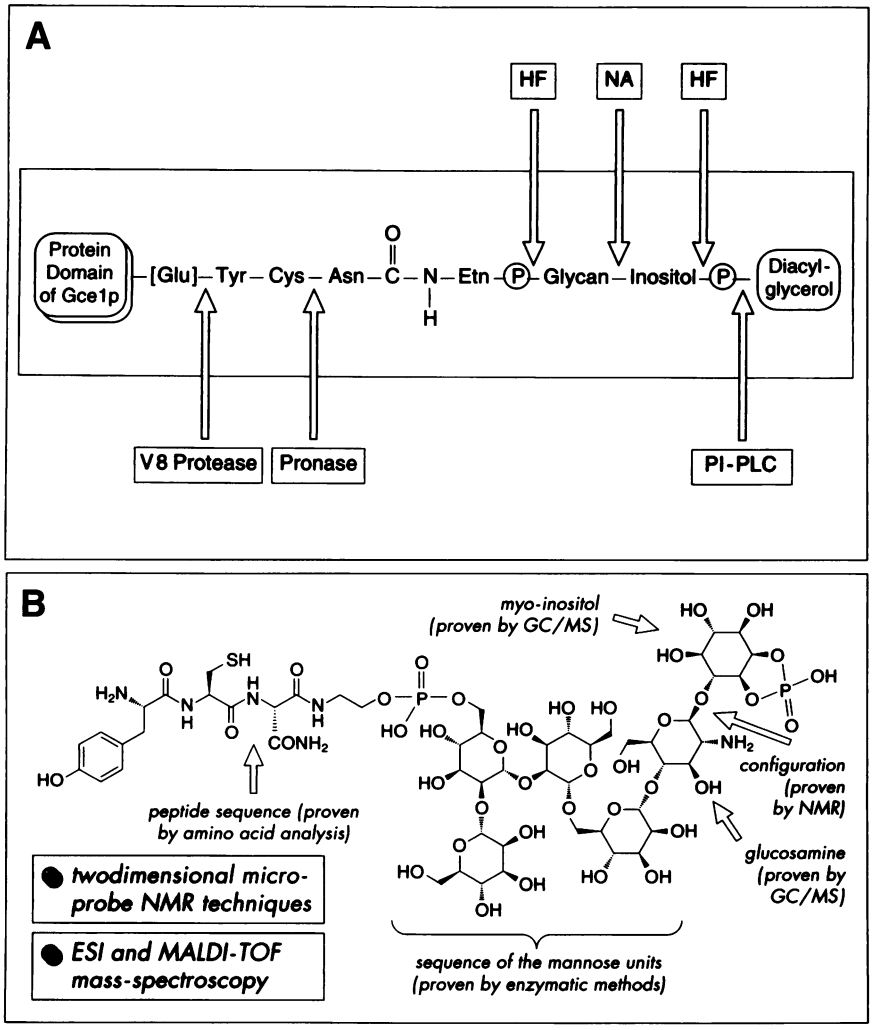

Fig. 1. Schema for the generation (A) and structure (B) of PIG-P. PIG-P is derived from the carboxy-terminal protein portion and GPI anchor of Gce1p from *Saccharomyces cerevisiae* by enzymatic cleavages in vitro with V8 protease from *Staphylococcus aureus* and PI-specific PLC from *Bacillus cereus*. The glycan portion consists of nonacetylated glucosamine glycosidically linked to a series of three mannose residues from which (the distal one) an additional mannose side chain can branch off (typical for yeast). The cleavage sites within the peptide portion for pronase and within the PIG portion for dephosphorylation of the two phosphodiester bridges by aqueous hydrogen fluoride (HF) or for deamination of the glucosamine residue by nitrous acid (NA) are indicated by arrows (A). The methods used for structural elucidation of special epitopes of the PIG-P are indicated (B) (24).

cellular systems, PIG-P stimulated lipogenesis in isolated rat adipocytes in a concentration-dependent manner to up to 90% of the maximal insulin effect (24). Its activity was slightly reduced in cells that had been desensitized for insulin action during primary culture of the adipocytes with high concentrations of glucosamine and insulin. PIG-P also activated glucose transport in isolated rat cardiomyocytes and adipocytes to up to 60% of the maximal insulin effect at concentrations in the low-micrometer range. The glucose transport activation was based on increased translocation of the glucose transporter isoform GLUT4 from internal stores, so-called low-density microsomes, or GLUT4 vesicles, to the plasma membrane, as has been amply documented for insulin (for a review see ref. 28). Furthermore, PIG-P regulated a number of key metabolic pathways and enzymes in an insulin-like fashion, e.g., it stimulated glycogen synthesis in the isolated rat diaphragm and inhibited protein kinase A in isolated rat adipocytes. The reduction in the protein kinase A activity ratio may represent the functional basis for the antilipolytic potency of PIG-P. Maximal effects were observed between 2 and 5 μm with EC_{50} values in the range of 0.3 to 0.5 μm (24).

A large body of evidence suggests, but does not prove, the involvement of GPI structures, GPI cleavage, or PIG molecules in metabolic insulin signaling. First, the partial insulin-mimetic metabolic activity of PIG molecules was inhibited by anti-PIG antibodies in cultured myocytes (29). Second, insulin stimulation of glycogen synthesis was abolished in mutant erythroleukemia cells with defective GPI synthesis (30). Third, PIG molecules exerted acute hypoglycemic activity in normal and streptozotocin diabetic rats (31). Fourth, PIG molecules were detected in human serum and their amount was reduced in

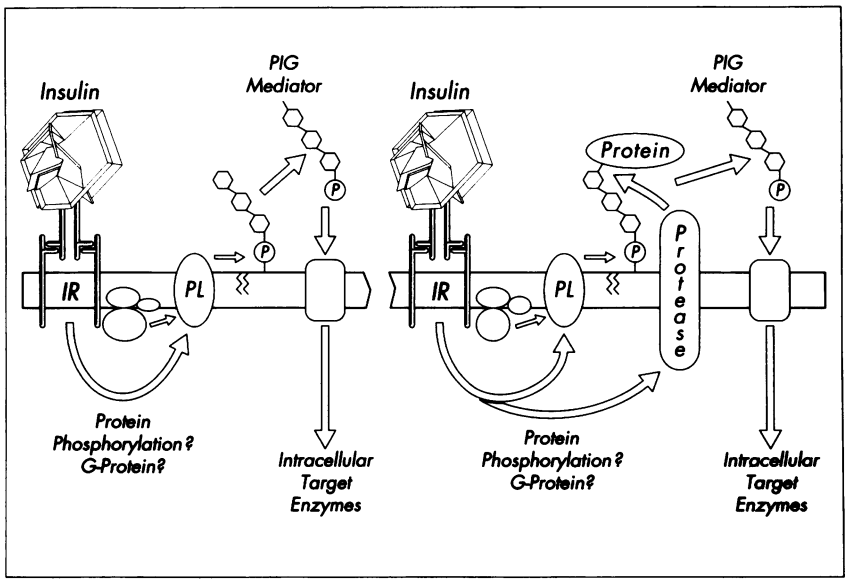

Fig. 2. Hypothetical model for the generation of soluble PIG molecules in insulin-sensitive cells from free GPI lipids. The GPI lipids are located at the extracellular leaflet of the plasma membrane by single lipolytic cleavage through a phospholipase (PL; left) or from GPI-anchored plasma membrane proteins by the combined actions of a phospholipase and protease (right). The PIG molecules are then transported across the plasma membrane through a channel or translocase (box). Possible modes for the regulation of the phospholipase and protease by the insulin receptor (IR) through phosphorylation and G proteins are indicated.

patients with non–insulin-dependent diabetes mellitus (NIDDM) (32,33). Finally, rat adipocytes made insulin resistant in vitro were impaired in insulin activation of the GPI-specific PLC (26). The partial insulin-mimetic activity of PIG structures in cellular and cell-free assay systems (34–43; for reviews see refs. 13,44,45) in combination with the possibility of the generation of PIG molecules from GPI structures (25,26,46,47) prompted Cuatrecasas et al. about 10 years ago to assign PIG molecules a function as soluble mediators of metabolic insulin action (19,48–50). According to this hypothesis (Fig. 2), PIG molecules are generated in response to insulin through lipolytic cleavage of free GPI lipids (Fig. 2, left) and/or GPI-anchored proteins (Fig. 2, right) by a PLC at the extracellular face of the plasma membrane of insulin-sensitive cells and are then transported into the cytosol, where they directly affect key metabolic enzymes and/or their regulatory proteins in an allosteric fashion.

An alternative model for the molecular mode of PIG action in insulin-sensitive cells is based on the putative function of caveolae as signaling compartments. It is interesting to note that in many cell types, including insulin-sensitive ones, a variety of GPI-anchored proteins, such as Thy-1 in lymphocytes and T cells (51, 52), and the bulk of GPI lipids are concentrated within so-called caveolae. Caveolae are small bulb- or flask-shaped invaginations or subcompartments/microdomains of the plasma membrane found in most cell types, but they are highly abundant in fibroblasts, adipocytes (20% of the total plasma membrane surface area), endothelial cells, epithelial cells, and smooth and skeletal muscle cells (for reviews see refs. 53,54). They are coated at the cytosolic face with the 21-kD membrane protein caveolin (55). The formation of caveolae may be promoted by the capacity of caveolin to form homo-oligomers by self-association (for a review see ref. 56). Caveolae are thought to be involved in various cellular transport processes (transcytosis, potocytosis, endocytosis, cholesterol flux; for reviews see refs. 53,54) and in transmembrane signal transduction events ("caveolae signaling hypothesis"; 57, 58). In addition to the "marker, coat or scaffolding" proteins, caveolin (three different tissue-specific isoforms have been identified so far) and the recently discovered flotillin (59), caveolae harbor a number of lipid-modified signaling molecules, such as small and heterotrimeric G proteins as well as nonreceptor tyrosine kinases of the Src family (for a review see ref. 60). The dual acylated version of these kinases partitions into the inner leaflet of the plasma membrane corresponding to the area of caveolae forming so-called detergent-insoluble complexes, which resist solubilization by 1% Triton X-100 in the cold (61,62). The close association with GPI-anchored proteins, caveolin, glycosphingolipids, glycolipids, and cholesterol enables the recovery of Src kinases together with these components in detergent-insoluble complexes (61–64; for a review see ref. 65). These possibly represent the

biochemical equivalent of caveolar structures, but this remains a matter of controversy.

In any case, the following lines of evidence hint at a role of caveolin, caveolae, and detergent-insoluble complexes in mediating or modulating signaling events by insulin, PIG and GPI molecules. *(1)* Caveolae are present in high numbers in insulin-sensitive cells (e.g., skeletal muscle cells [66]). *(2)* The expression level of caveolin directly correlates with the morphological appearance of caveolae during differentiation of 3T3-L1 fibroblasts into adipocytes, which is accompanied by a gain of insulin sensitivity (55, 67). *(3)* GLUT4 is associated with caveolin-rich vesicles in 3T3-L1 adipocytes (67). *(4)* GPI lipids are found to be localized in specific plasma membrane structures, referred to as caveolae in 3T3-L1 adipocytes (68). *(5)* GLUT4 seems to be translocated to caveolae of the plasma membrane in response to insulin in 3T3-L1 adipocytes (67,69; this, however, is still controversial; see refs. 70,71). *(6)* The activated or autophosphorylated insulin receptor appears to be enriched in caveolae of rat adipocytes (S. Gustavsson, B. Borg, S. Larsson, M. Parpal, K. Magnusson, P. Stralfors, unpublished results. *(7)* Insulin, but not epidermal growth factor (EGF) or platelet-derived growth factor (PDGF) stimulates tyrosine phosphorylation of caveolin in 3T3-L1 adipocytes (72).

However, both the "mediator" as well as the "caveolae" model for insulin-mimetic PIG action has remained speculation as essentially no data are presently available concerning the molecular targets and signaling events triggered by PIG molecules. Such an analysis has been hampered by the limited amounts, heterogeneous nature, ill-defined structure, and concentration of the PIG preparations available thus far. We therefore used the structurally defined PIG-P from yeast Gce1p to study the molecular mechanism of PIG action in insulin-sensitive cells and to attempt a differentiation between the two proposed models.

Materials and Methods

Materials

PIG-P was prepared from the core glycan of Gce1p from *S. cerevisiae*, purified to radiochemical and chemical homogeneity, and quantitated as described previously (24). The sulfonylureas glimepiride and tolbutamide, and semisynthetic human insulin (I81 0182) were synthesized by the chemical synthesis department of Hoechst Marion Roussel Deutschland GmbH, Frankfurt am Main, and dissolved as described previously (73). PD098059 was purchased from BioMol, Hamburg, Germany; LY294002, rapamycin, and PI-specific PLC from *B. cereus* were supplied by Calbiochem, Bad Soden, Germany. TPCK-treated trypsin from bovine pancreas (type XIII), trypsin inhibitor from soybean (type I-S), V8 protease from *S. aureus*, and PC-specific PLC from *Chlostridium perfringens* (type XIV) were from Sigma, Deisenhofen, Germany. NEM was obtained from Pierce, Rockford, IL, and protease inhibitors were purchased from Boehringer Mannheim, Germany. Male Wistar rats (60–80 g and 140–160 g) were provided by the animal breeding station of Hoechst Marion Roussel Deutschland GmbH. Radiochemicals were purchased as described previously (23–27; 73–75) unless indicated otherwise. All other materials were obtained from Merck, Darmstadt, Germany and were of the highest purity available.

Preparation of Isolated Rat Adipocytes and Diaphragms and Incubation with PIG-P/insulin

Adipocytes were isolated from epididymal fat pads of male rats (140–160 g) by digestion with collagenase as outlined previously (73, 74). Released adipocytes were washed three times with Krebs-Ringer phosphate (KRP)-Hepes (140 mM NaCl, 5 mM KCl, 1.25 mM $MgSO_4$, 2 mM $CaCl_4$ 10 mM Na_2HPO_4, 25 mM Hepes salt-free acid, pH 7.4, 2% BSA) containing 5 mM glucose by flotation and then suspended in KRP-Hepes containing 50 μm glucose and 1 mM sodium pyruvate (at 3.5×10^5 or 1×10^6 cells/ml, respectively) for incubation (20 min, 37°C) in the absence or presence of PIG-P/insulin in a gently shaking waterbath in an atmosphere of 95% O_2/5% CO_2. Intact diaphragms (with rib cage attached) were prepared from rats (60–80 g) and separated into hemidiaphragms as described previously (24, 75). The washed hemidiaphragms were incubated (30 min, 30°C) with PIG-P/insulin at the concentrations indicated in 20 ml of Krebs-Ringer (KRO) buffer (140 mM NaCl, 6 mM KCl, 2 mM $CaCl_2$, 1 mM $MgSO_4$ 1.2 mM $KHPO_4$, 0.1% BSA, 25 mM Hepes/KOH, pH 7.4) containing 5 mM glucose and 1 mM sodium pyruvate and equilibrated with O_2 (with one change of buffer after 15 min) through continuous bubbling with O_2 and mild shaking. Subsequently, the diaphragms were washed with KRO buffer containing 2 mM pyruvate and 5 mM

sucrose, incubated in 20 ml of the same buffer supplemented with PIG-P/insulin for 10 min, and finally washed with KRO buffer containing 2 mM pyruvate, 1 mM deoxyglucose, and 4 mM sucrose.

Assays for Lipogenesis, Glucose Transport, and Glycerol-3-phosphate Acyltransferase (GPAT)

Lipogenesis was determined as incorporation of [^{3}H]glucose into total toluene-extractable lipids according to Müller et al. (74). Briefly, 0.2 ml of adipocyte suspension (3.5×10^5 cells/ml) was incubated (90 min, 37°C) in 1 ml of KRP-Hepes containing 1 mM sodium pyruvate and 50 μm [3-^{3}H]glucose (DuPont-New England Nuclear, Bad Homburg, Germany; 10 Ci/mmol, 0.4 μCi) in the absence or presence of PIG-P/insulin in a gently shaking waterbath in an atmosphere of 95% O_2/5% CO_2. Glucose transport in adipocytes was assayed by incubation of 0.5×10^6–cell portions in 1 ml of KRP-Hepes containing 1 mM sodium pyruvate and 0.1 mM 2-deoxy[2,6-^{3}H]glucose (Amersham-Buchler, Braunschweig, Germany; 25 Ci/mmol, 0.5 μCi) in the absence or presence of PIG-P/insulin for 5 min at 22°C. Further processing by centrifugation through an oil cushion and calculation were done as outlined previously (24, 74). Glucose transport in diaphragms was assayed by incubation of hemidiaphragms in 20 ml of KRO buffer containing 2 mM pyruvate, 1 mM 2-deoxy[2,6-^{3}H]glucose (5 μCi), and 4 mM [U-^{14}C]sucrose (Amersham-Buchler, Braunschweig, Germany; 20 mCi/mmol, 5 μCi) in the absence or presence of PIG-P/insulin for 20 min at 30°C under continuous bubbling with O_2 and mild shaking. Further processing and calculation were performed as described previously (24). GPAT recovered with a crude microsomal fraction from isolated adipocytes (prepared by centrifugation [150,000 × *g*, 60 min] of the supernatant, which had been obtained by centrifugation [14,000 × *g*, 20 min] of a fat-free homogenate) was assayed as incorporation of [^{3}H]glycerol-3-phosphate into butanol-extractable lipids according to Müller et al. (76). Briefly, 100 μg of microsomal protein was incubated (3 min, 37°C) in 0.5 ml of 0.2 mM [2-^{3}H]glycerol-3-phosphate (Biotrend, Cologne, Germany; 10 Ci/mmol, 0.5 μCi), 150 μm palmitoyl-CoA, 250 mM sucrose, 0.5 mM EDTA, 1 mM dithiothreitol (DTT), 0.1 mM phenylmethylsulfonyl fluoride (PMSF), and 25 mM Tris/HCl (pH 7.4).

Metabolic Labeling of Adipocytes with [^{35}S]methionine

Isolated rat adipocytes (2×10^7 cells) were suspended in 40 ml of Dulbecco's minimal essential medium (DMEM) containing 10 mM glucose and 2% BSA and depleted of methionine in 400-ml plastic containers. They were then incubated (1 hr, 37°C) in the presence of 10 nM insulin prior to addition of 100 μCi L-[^{35}S]methionine (Amersham-Buchler, Braunschweig, Germany, 1000 Ci/mmol). After further incubation for 2 hr under mild shaking, the adipocytes were separated from the medium by flotation and then resuspended in 10 ml of KRP-Hepes containing 5 mM glucose for preparation of trypsin/salt extract.

Preparation of Detergent-Insoluble Complexes

FROM DIAPHRAGMS. Six rat hemidiaphragms were homogenized in 25 ml of ice-cold 25 mM Hepes/potassium hydroxide (KOH) (pH 7.4), 250 mM sucrose, 4 mM EDTA, 30 mM sodium pyrophosphate, 50 mM NaF, 1 mM Na_3VO_4, 0.2 mM PMSF, 25 mM benzamidine, 2 μm leupeptin, 5 μm pepstatin, and 2.5 trypsin inhibitory unit/milliliter aprotinin by using a Polytron (setting 6, 2 × 30 sec) and subsequently a Teflon-in-glass homogenizer (15 strokes, 1500 rpm, 4°C). The homogenates were centrifuged (5000 × *g*, 20 min, 4°C). The supernatants were adjusted to 0.8 M KCl, incubated (30 min, 4°C), and then centrifuged (200,000 × *g*, 90 min, 4°C). The total membrane pellet was suspended in 2 ml of 0.1 M Tris/HCl (pH 6.5), 150 mM NaCl, 1% TX-100, 30 mM sodium pyrophosphate, 50 mM NaF, 1 mM Na_3VO_4, 1 mM PMSF, 2 μm leupeptin, and 5 μm pepstatin and repeatedly passed through a 25-gauge needle. The extract was adjusted to 40% sucrose by addition of 2 ml of 80% sucrose in the same buffer.

FROM ADIPOCYTES. A portion of 3.5×10^6 cells was washed three times with phosphate-buffered saline (PBS), suspended in 3 ml of 25 mM Mes/KOH (pH 6.5), 150 mM NaCl, 1% TX-100, 30 mM sodium pyrophosphate, 50 mM NaF, 1 mM Na_3VO_4, 1 mM PMSF, 2 μm leupeptin, and 5 μm pepstatin and then homogenized in a Teflon-in-glass homogenizer (10 strokes, 500 rpm, 4°C). After centrifugation (500 × *g*, 1 min), 2 ml of infranatant consisting of total fat-free extract was adjusted to 40% sucrose by addition of 2 ml

of 80% sucrose in the same buffer. The diaphragm and adipocyte extracts were placed at the bottom of an ultracentrifuge tube and then overlaid with 8 ml of a linear 5–30% sucrose gradient (in 0.1 M Tris/HCl, pH 6.5, 1 mM Na_3VO_4, 1 mM PMSF, 2 μm leupeptin, and 5 μm pepstatin) lacking TX-100. The gradients were centrifuged (Beckman SW41 rotor, 39,000 rpm, 16 hr, 4°C). Detergent-insoluble complexes, which fractionated as a sharp, light-scattering band at a density of 15–20% sucrose (77,78), were diluted with five volumes of 0.1 M Tris/HCl (pH 6.5), 1 mM Na_3VO_4, 50 mM NaF, 30 mM sodium pyrophosphate, 1 mM PMSF, 2 μm leupeptin, and 5 μm pepstatin and collected by centrifugation (250,000 × *g*, 1 hr, 4°C).

Tyrosine Phosphorylation of Caveolin

The collected detergent-insoluble complexes were solubilized in 1 ml of TEST buffer (50 mM Tris/HCl, pH 7.4, 150 mM NaCl, 1 mM EDTA, 1 mM Na_3VO_4, and 1% TX-100) or 1 ml of 20 mM Tris/HCl (pH 8.0), 150 mM NaCl, 1% TX-100, 60 mM octylglucoside, 1 mM Na_3VO_4, 20 μg/ml aprotinin, and 10 μg/ml leupeptin (1 hr, 4°C). The supernatant of a subsequent centrifugation (15,000 × *g*, 10 min, 4°C) was precleared with protein A-Sepharose and then immunoprecipitated with 5 μl (10 μg) of rabbit anti-caveolin antibodies (that recognize the rat caveolin 1 epitope consisting of residues 38–49; Transduction Laboratories, Lexington, KY). Following incubation (4 hr, 4°C) and addition of 100 μl of protein A–Sepharose (50 mg/ml) and further incubation (16 hr, 4°C), the immunocomplexes were collected by centrifugation (15,000 × *g*, 2 min, 4°C), washed twice with TEST buffer, and three times with TEST buffer lacking TX-100, dissolved in 50 μl of 2-fold Laemmli sample buffer containing 8 M urea and lacking mercaptoethanol (5 min, 95°C), and finally separated by reducing SDS-PAGE (8.5% resolving gel). Proteins were transferred to polyvinylidene difluoride (PVDF) membranes (Schleicher & Schüll, Dassel, Germany) in buffer consisting of 20% methanol, 200 mM glycine, and 25 mM Tris/HCl (pH 8.3). Following transfer (the efficiency of which was confirmed by Coomassie blue staining of the gel after the electroblot), the filters were blocked with 5% nonfat dry milk, 0.1% Tween 20, and 0.02% sodium azide in PBS for 1 hr at 37°C and then incubated with monoclonal anti-phosphotyrosine antibody 4G10 (at a dilution of 1:500 to 1:1000; Upstate Biotechnologies, Lake Placid, NY). Visualization of the immune complexes was performed using [^{125}I]protein A (3000 Ci/mmol, Amersham-Buchler, Braunschweig, Germany). The radiolabeled blots were evaluated by phosphorimaging (Molecular Dynamics, Storm 840, Gelsenkirchen, Germany) and Molecular Analyst Version 2.1.1 software (Bio-Rad, Munich, Germany). The amounts of the 21-kD and 24-kD forms of caveolin (presumably differing in the codon used for initiation of translation [72]) were added up.

Protease and Salt Treatment of Rat Adipocytes

Ten milliliters of adipocyte suspension (3.5×10^5 cells/ml) in KRP-Hepes containing 5 mM glucose was supplemented with an appropriate volume of a trypsin stock solution (10 mg/ml) to the desired concentration and incubated (20 min, 30°C) in 50-ml Falcon tubes under rotation. After addition of a 4-fold volume of trypsin inhibitor stock solution (10 mg/ml) and 10 ml of KRP-Hepes containing or lacking (control) 1 M NaCl and further incubation (10 min, 22°C), the cells were centrifuged (1500 × *g*, 5 min, swing-out rotor). For washing of the cells, the infranatant was removed and the remaining cell suspension (about 1 ml) was supplemented with 50 ml of KRP-Hepes, gently mixed, and then centrifuged again (500 × *g*, 1 min, swing-out rotor). After two additional washing steps, the final cell suspension was adjusted to 10 ml of KRP-Hepes containing 50 μm glucose and 1 mM sodium pyruvate. Portions of 0.2 ml were used for the lipogenesis assay. Control cells (no treatment with trypsin) received water instead of trypsin and were subjected to the same centrifugation and washing procedures as the trypsin-treated cells.

Preparation, Pretreatment, and Radiolabeling with N-ethylmaleimide (NEM) of the Trypsin/Salt Extract

For preparation of the extract from intact adipocytes, 25 ml of adipocyte suspension (2.5×10^6 cells/ml) in KRP-Hepes containing 5 mM glucose was incubated (20 min, 22°C) with up to 500 μl of trypsin stock solution (10 mg/ml) or water in 50-ml Falcon tubes under rotation. After addition of up to 2 ml of trypsin inhibitor (10 mg/ml), 1 mM PMSF, 25 mM benzamidine, 2 μm leupeptin, 5 μm pepstatin, and 10 μg/ml antipain or

water and 27.5 ml of 1 M NaCl in KRP-Hepes, the cells were centrifuged (1500 × *g*, 5 min, swing-out rotor). The infranatant was removed, dialyzed for 16 hr against 4 × 500 ml of ice-cold HEG buffer (25 mM Hepes/KOH, pH 7.4, 1 mM EDTA, 5% glycerol, 0.2 mM PMSF) and then supplemented with the same volume of ice-cold 25% polyethylene glycol (PEG) 6000 in the same buffer. After incubation (2 hr, 4°C), the precipitates were collected by centrifugation (48,000 × *g*, 30 min, 4°C), washed twice with 6% polyethylene glycol 6000, and then frozen and stored in liquid nitrogen until use. For the reconstitution experiments, the precipitates (corresponding to 4000 arbitrary units) were dissolved in 4 ml or 400 μl (10-fold concentrated) of HEN buffer (25 mM Hepes/KOH, pH 7.4, 1 mM EDTA, 1 M NaCl). Control extracts were prepared by treatment of the adipocytes with trypsin alone (addition of water instead of NaCl), or NaCl alone (addition of water instead of trypsin), or V8 protease (250 μg/ml final concentration) in the presence of NaCl with subsequent procedures performed as described for the trypsin/salt extract.

For preparation of the trypsin/salt extract from detergent-insoluble complexes, 1-mg portions of detergent-insoluble complexes (prepared as described above) were suspended in 2.5 ml of 20 mM Tris/HCl (pH 8.0), 0.5 mM EDTA, and 0.1% TX-100 and incubated (30 min, 15°C) in the presence of 60 μg/ml trypsin. After addition of 200 μl of trypsin inhibitor stock solution (see above) and 2.7 ml of NaCl in 20 mM Tris/HCl (pH 8.0), omitted for preparation of trypsin extract alone, the complexes were centrifuged (200,000 × *g*, 75 min, 4°C). The supernatant was dialyzed for 16 hr against 2 × 100 ml of ice-cold HEG buffer, then supplemented with the same volume of 25% PEG 6000 and further processed as described above. For reconstitution experiments, the precipitates (corresponding to 1000 arbitrary units) were dissolved in 1 ml or 100 μl (10-fold concentrated) of HEN buffer.

For pretreatment of the trypsin/salt extract, 200-μl portions of extract were heated (15 min, 100°C) or incubated with 20 μg proteinase K (60 min, 4°C) and then with 1 mM PMSF (5 min, 4°C) or incubated with NEM (1.5 mM final concentration, 30 min, 25°C) and then with DTT (15 mM final concentration, 5 min, 4°C) or incubated with 150 μg V8 protease (60 min, 4°C) and then PMSF (1 mM final concentration, 5 min, 4°C) in a total volume of 250 μl. All samples were subsequently precipitated by addition of 250 μl of 25% PEG 6000. Further processing of the precipitates was as described above. For dialysis (using Spectra/Por, molecularporous membrane, MWCO 10,000; Roth, Karlsruhe, Germany), 1 ml of extract was dialyzed against 200 ml of HEN buffer containing 5% glycerol (16 hr, 4°C). Control pretreatments were performed with the corresponding buffers lacking the reagents but with the authentic termination reactions, incubation periods, and precipitations.

For radiolabeling of the extract with NEM, portions of the extract were precipitated with PEG 6000, solubilized in 200 μl of HEN buffer, and incubated (30 min, 25°C) with 20 μCi *N*-ethyl[2,3-^{14}C]maleimide (10 mCi/mmol) in the absence or presence of 50 mM DTT. Subsequently, the samples were precipitated with trichloroacetic acid (TCA) (5% final concentration) and then washed (twice with acetone) precipitates were analyzed by SDS-PAGE and fluorography.

Reconstitution of Trypsin/Salt–Treated Adipocytes with Trypsin/Salt Extract

Two hundred-fifty microliters of extract (normal or 10-fold concentrated) or the volumes indicated (and adjusted to 250 μl with water) were added to 0.3-ml portions of adipocyte suspension (3.5 × 10^5 cells/ml of KRP-Hepes containing 5 mM glucose) in 10-ml plastic tubes. The reconstitution was initiated by supplementation with 1.95 ml of KRP-Hepes containing 5 mM glucose. After incubation (1 hr, 22°C) under rotation at 60 rpm in a temperature-controlled tube roller with an atmosphere of 95% O_2/5% CO_2, the cells were centrifuged (500 × *g*, 1 min), washed twice with KRP-Hepes, and suspended in 0.2 ml of KRP-Hepes containing 50 μm glucose and 1 mM sodium pyruvate for assaying lipogenesis or glucose transport. In some experiments, the washing cycles (1500 × *g*, 5 min) were performed with KRP-Hepes containing 0.3 or 0.7 M NaCl and finally, with salt-free KRP-Hepes.

Miscellaneous Procedures

SDS-PAGE in the presence of urea and fluorography was performed according to published procedures (79).

Results

Analysis of Signaling Pathways for Metabolic PIG-P Actions Downstream of Insulin Receptor Substrate-1 (IRS-1)

Tyrosine phosphorylation of IRS-1 by the activated insulin receptor kinase has been recognized to represent an early step of insulin signaling. We therefore previously investigated whether this segment of the insulin signaling cascade is modified by PIG-P and if additional phosphoproteins might be affected using isolated rat cardiomyocytes (80). These studies demonstrated that PIG-P stimulates tyrosine phosphorylation of IRS-1 and activates PI 3-kinase in a rapid and reversible manner to up to 60% of the maximal insulin activity. However, unlike the situation with insulin, PIG-P action did not depend on the functional insulin receptor and failed to induce its tyrosine phosphorylation.

To determine whether the activation of PI 3-kinase by PIG-P is indeed functionally linked to glucose transport activation by the compound, we used the specific PI 3-kinase inhibitor, LY294002 (81). Isolated rat diaphragms (Fig. 3A) or adipocytes (Fig. 3B) were incubated with increasing concentrations of LY294002 for 5 min before addition of insulin or PIG-P. After a 15-min incubation, glucose uptake was assayed. In diaphragms and adipocytes, LY294002 produced a concentration-dependent inhibition of glucose transport activation by both PIG-P and insulin with comparable IC_{50} values. Basal transport was hardly affected. In contrast, essentially no inhibition of PIG-P and insulin-stimulated glucose transport in diaphragms (data not shown) and adipocytes (Fig. 4A) was found after blockade of the p70S6kinase by the inhibitor rapamycin (82) and blockade of the MAPK kinase by the inhibitor PD098059 (83) (Fig. 4B).

Next we studied whether the activation of the key metabolic enzyme of lipid synthesis, GPAT, by PIG-P in adipocytes involves the stimulation of PI 3-kinase, p70S6kinase, or MAPK kinase. Isolated rat adipocytes were incubated with increasing concentrations of the corresponding inhibitors, LY249002, rapamycin, and PD098059, respectively, for 5 min prior to addition of PIG-P (5 μm final concentration). After further incubation for 15 min, the cells were assayed for GPAT activity in vitro by incubating a crude microsomal fraction with [^{3}H]glycerol-3-phosphate. Quantitative evaluation of the butanol-extracted radiolabeled lipid products by thin-layer chromatography (TLC) analysis and radioactivity scanning of the plates (Fig. 5) revealed that the activation of GPAT by PIG-P (to up to 85% of the maximal insulin effect at 5 μm) was concentration-dependently inhibited by both LY294002 (Fig. 5A) and rapamycin (Fig. 5B), but remained almost unaffected by PD098059 (data not shown). The inhibitors did not significantly reduce basal GPAT activity. The EC_{50} values of LY294002 and rapamycin, respectively, were very similar for inhibition of the PIG-P- and insulin-induced activation of GPAT. Thus, PIG-P and insulin appear to regulate GPAT by similar mechanisms downstream of PI 3-kinase involving activation of p70S6kinase. Obviously, the signals for stimulation of glucose transport and GPAT triggered

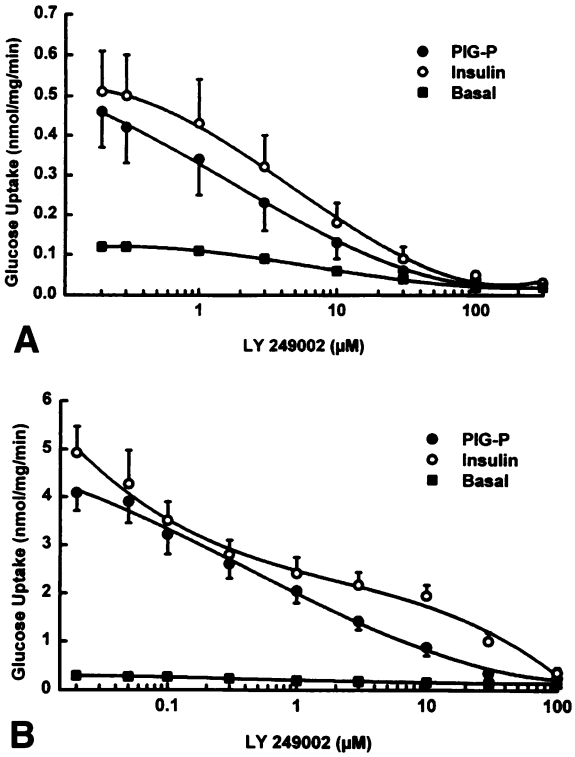

Fig. 3. Effect of the inhibition of PI 3-kinase on glucose transport activation by PIG-P in isolated rat diaphragms (A) and adipocytes (B). Diaphragms and adipocytes were treated with increasing concentrations of LY294002 for 5 min prior to incubation in the absence (basal) or presence of PIG-P (5 μm) and insulin (10 nM for adipocytes, 100 nM for diaphragms) for 20 min and then assayed for glucose transport. Each point represents the mean ± SD of at least three different adipocytes or diaphragm preparations and incubations, with transport measurements in quadruplicate.

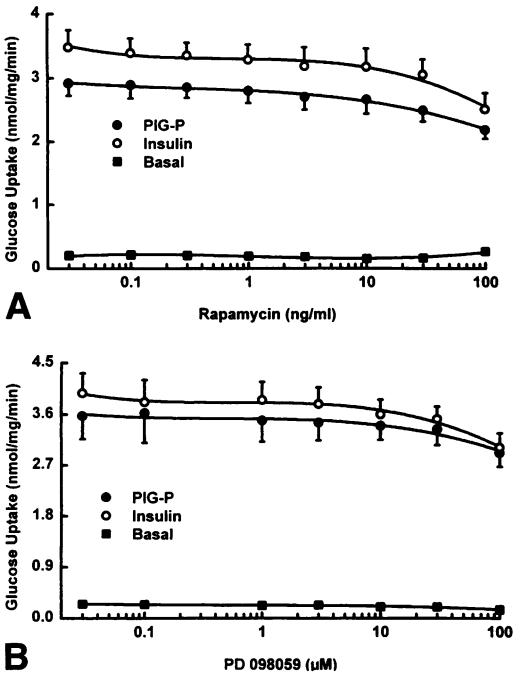

Fig. 4. Effect of the inhibition of p70S6kinase (A) and MAPK kinase (B) on glucose transport activation by PIG-P in isolated rat adipocytes. The experiment was performed as described in the legend to Fig. 3 using rapamycin (A) and PD098059 (B), respectively.

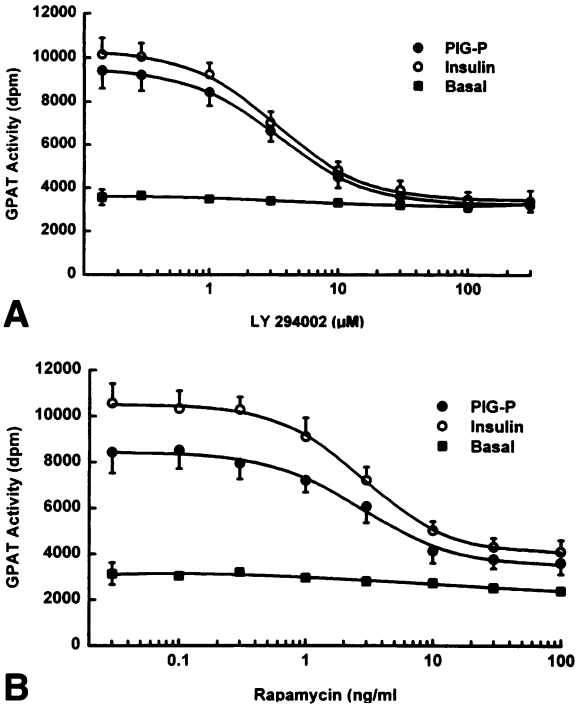

Fig. 5. Effect of the inhibition of PI 3-kinase (A) and p70S6kinase (B) on activation of GPAT by PIG-P in adipocytes. Isolated rat adipocytes were treated with increasing concentrations of LY294002 (A) or rapamycin (B) for 5 min prior to incubation (20 min, 37°C) in the absence (basal) or presence of PIG-P (5 μm) or insulin (10 nM) and then assayed for GPAT activity. Each point (dpm-values of the butanol-extracted and TLC-separated radiolabeled lipid products) represents the mean ± SEM of four different cell preparations and incubations, with activity measurements in triplicate.

by both PIG-P and insulin diverge downstream of activated PI 3-kinase (which is required for both glucose transport and GPAT) and upstream of activated p70S6kinase (which is required for GPAT only). It will be interesting to see whether protein kinase B and glycogen synthase kinase 3, which are both located downstream of PI 3-kinase and known to be activated and inactivated, respectively, in response to insulin (for a review see ref. 84) and PIG molecules (W. Frick, A. Bauer, J. Bauer, S. Wied, S. Welte, G. Müller, unpublished results) participate in the regulation of glucose transport and GPAT by these stimuli. The study of this question, however, will require the development of specific inhibitors for those enzymes. In conclusion, insulin and PIG-P signaling seems to be divergent upstream of IRS-1 but converges at the level of PI 3-kinase. PIG-P will circumvent insulin resistance if the defect is located upstream of PI 3-kinase. This might be the case in isolated adipocytes desensitized for insulin action by long-term incubation with high concentrations of glucosamine and insulin (73,80).

Analysis of Initial Steps of Metabolic Signaling by PIG-P

In a first attempt to identify cell-surface components required for signaling by PIG-P, e.g., for stimulation of lipogenesis, we looked for conditions for desensitization of isolated rat adipocytes toward PIG-P action. The adipocytes were incubated with increasing concentrations of trypsin. After termination of the digestion and subsequent washing and re-isolation of the cells by flotation, the adipocytes were assayed for stimulation of lipogenesis by PIG-P and sodium vanadate. Vanadium compounds are known to exert insulin-mimetic activity on isolated adipocytes via interference with unknown intracellular sites, presumably the inhibition of certain protein tyrosine phosphatases and/or activation of certain cytosolic tyrosine kinases (for reviews see refs. 85,86).

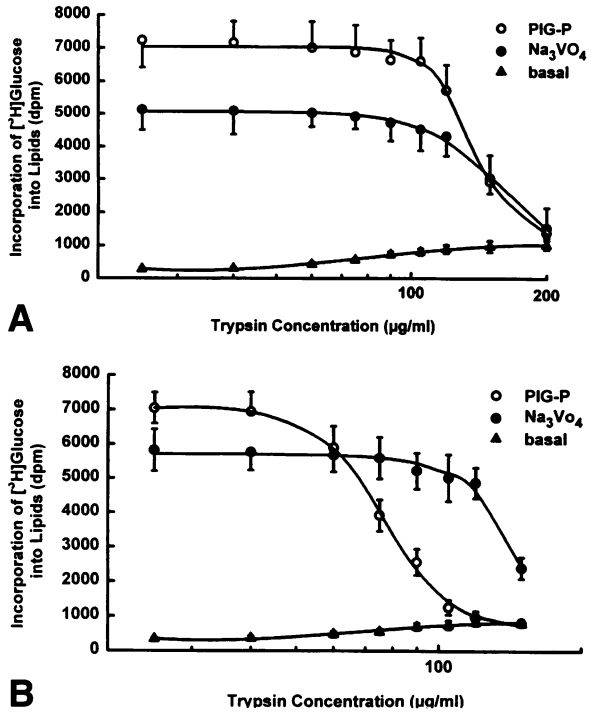

Fig. 6. Effect of trypsin and salt treatment of adipocytes on stimulation of lipogenesis by PIG-P. Isolated rat adipocytes were treated with increasing concentrations of trypsin (as described in Materials and Methods). After termination of the digestion and further incubation for 10 min in the absence (A) or presence of 0.5 M NaCl (B), the washed cells were treated with PIG-P (5 µm) or sodium vanadate (1 mM) or left untreated (basal) and then assayed for lipogenesis. Each point (dpm values of toluene-extractable radiolabeled lipid products) represents the mean ± SD of at least three different adipocyte preparations and trypsin treatments, with lipogenesis measurements in duplicate.

Concentrations up to 120 µg/ml trypsin did not significantly affect the stimulation of lipogenesis by either PIG-P (5 µm) or sodium vanadate (1 mM) (Fig. 6A). At higher concentrations, the insulin-mimetic activity of both compounds was drastically reduced with comparable dependence on the trypsin concentration. Thus, no differentiation between the actions of PIG-P and sodium vanadate was achieved by trypsin treatment of the adipocyte surface alone. The decrease in sensitivity of the cells toward both PIG-P and sodium vanadate at higher concentrations of trypsin is best explained by a general loss of cell viability. Next, the adipocytes were washed with 0.5 M NaCl following trypsin digestion prior to the lipogenesis assay. Now a clear-cut differentiation between the PIG-P and vanadate actions was observed (Fig. 6B). At 120 µg/ml trypsin, stimulation of lipogenesis by PIG-P was reduced to <10% of that obtained with mock-treated control cells. In contrast, this trypsin concentration did not significantly impair the insulin-mimetic activity of sodium vanadate. Obviously, the combination of trypsin and salt treatment, but not either treatment alone, of intact adipocytes led to inactivation of a component at the extracellular face of the plasma membrane, which is required for PIG-P but dispensable for vanadate action.

This was confirmed by studying the concentration–response curves of PIG-P for stimulation of lipogenesis in adipocytes that had been subjected to a combined trypsin/salt treatment (Fig. 7A). Very similar curves were obtained for cells treated with trypsin (100 µg/ml) alone, salt (0.5 M NaCl) alone, and mock-treated adipocytes (data not shown). This trypsin treatment, however, led to complete desensitization of the cells toward insulin action, presumably caused by cleavage of the insulin receptor (data not shown, see also ref. 24). In contrast, washing of the trypsin-treated adipocytes with 0.5 M NaCl caused a reduction in both the maximal responsiveness for PIG-P (measured at 20 µm) and sensitivity toward PIG-P (measured as EC_{50} value), the degree of which was dependent on the trypsin concentration used (Fig. 7A). At 100 µg/ml trypsin, 20 µm PIG-P almost completely failed to stimulate lipogenesis in salt-washed adipocytes. The dependence of the efficiency of the combined trypsin/salt treatment on the concentration of NaCl used for washing of the trypsinized adipocytes is demonstrated in Figure 7B. Half-maximal and complete inhibition of PIG-P-stimulated lipogenesis was achieved with about 250 mM and 750 mM NaCl, respectively (Fig. 7B, circles). Treatment of the adipocytes with NaCl alone over the total concentration range did not lead to an increase in basal lipogenesis (Fig. 7B, filled squares) or a decrease in PIG-P-stimulated lipogenesis (Fig. 7B, open squares). Thus the washing of the cells prior to lipogenesis seems to be quite efficient in reducing the salt concentration from 1 M at maximum below values deleterious for basal or activated lipogenesis. At these concentrations of NaCl and at 100 µg/ml trypsin during the incubation period, the viability of the cells was not significantly impaired, as judged from the release of lactate dehydrogenase and the stimulation of lipogenesis by sodium vanadate (data not shown). The curious requirement of both proteolytic cleavage and high ionic strength for

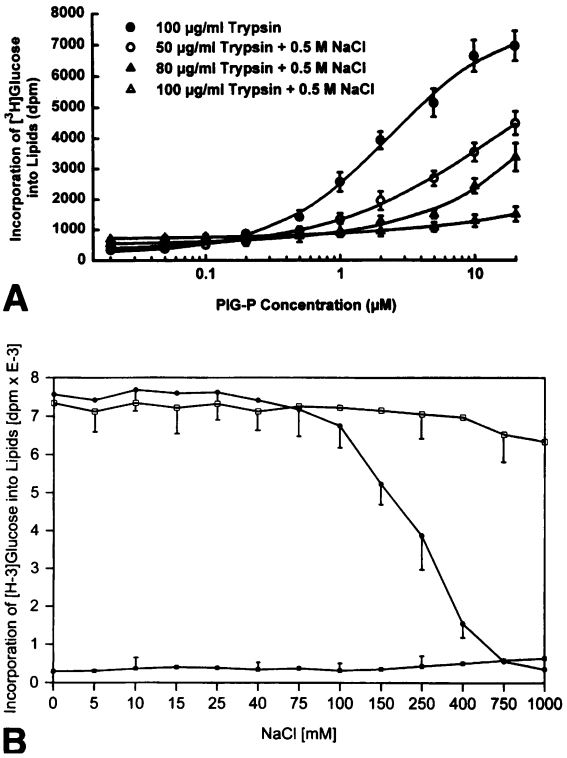

Fig. 7. Effect of combined trypsin/salt treatment of adipocytes on stimulation of lipogenesis by PIG-P. Isolated rat adipocytes were treated (20 min, 22°C) with the indicated concentrations of trypsin (A) or 100 µg/ml trypsin (B, circles) or left untreated (B, open and filled squares). After termination of the digestion and subsequent incubation in the absence or presence of 0.5 M NaCl (A) or the indicated concentrations of NaCl (B), the washed cells were treated with increasing concentrations of PIG-P (A) or with 5 µm PIG-P (B, circles and open squares) or left untreated (B, filled squares) and then assayed for lipogenesis. Each point represents the mean ± SEM of two adipocyte preparations and trypsin treatments, with lipogenesis measurements in quadruplicate.

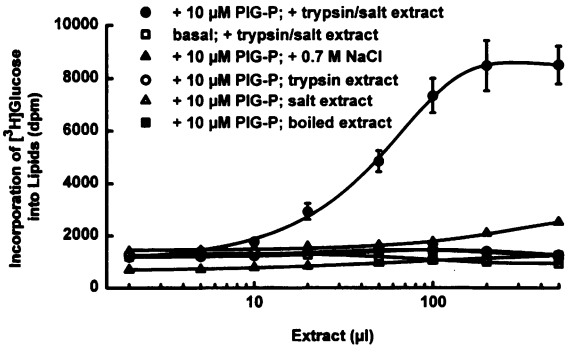

Fig. 8. Effect of the addition of trypsin/salt extract to trypsin/salt–treated adipocytes on stimulation of lipogenesis by PIG-P. Isolated rat adipocytes were treated (20 min, 22°C) with 100 µg/ml trypsin and subsequently with 0.5 M NaCl. The washed cells were supplemented with increasing volumes of trypsin/salt extract, trypsin extract, salt extract, or boiled trypsin/salt extract (prepared as described in Materials and Methods) and then diluted 10-fold or adjusted to 0.7 M NaCl. After further incubation (1 hr, 22°C), the cells were washed three times by flotation, incubated in the absence (basal) or presence of PIG-P (10 µm) and then assayed for lipogenesis. Each point represents the mean ± SD of three adipocyte preparations and reconstitution reactions, with lipogenesis measurements in quadruplicate.

desensitization of adipocytes toward PIG-P may be explained by involvement in PIG-P action of a proteinaceous component that is associated with the plasma membrane through a transmembrane domain and additional bipolar interactions between its extracellular domain and the plasma membrane.

To substantiate this hypothesis and to obtain a functional assay for purification of this component putatively contained in the trypsin/salt extract, we tried to restore the sensitivity of trypsin/salt–treated adipocytes, i.e., desensitized adipocytes, toward PIG-P action by the addition of trypsin/salt extract to these cells. The proteins constituting the trypsin/salt extract were dialyzed, precipitated, and dissolved in a buffer containing 1 M NaCl prior to addition to isolated adipocytes, which had been inactivated for PIG-P action by pretreatment with 100 µg/ml trypsin and subsequent salt wash. The reconstitution reaction was initiated by a 10-fold dilution of the mixture and further incubation. The adipocytes were separated from the incubation medium by three flotation cycles and finally assayed for stimulation of lipogenesis by PIG-P (Fig. 8). The addition of increasing volumes of trypsin/salt extract to the trypsin/salt–treated adipocytes caused restoration of PIG-P-stimulated lipogenesis, i.e., the formerly desensitized adipocytes regained sensitivity toward PIG-P. Control extracts prepared by trypsin or salt treatment alone or boiled trypsin/salt extract completely failed to reconstitute PIG-P action, as was the case for the presence of 0.7 M NaCl during the reconstitution reaction.

The concentration–response curves for activation of lipogenesis by PIG-P using reconstituted adipocytes revealed that these cells exhibit 65–75% of the response compared with that of mock-treated control cells with very similar EC_{50} values of 2 to 5 µm (Fig. 9A). In addition to the

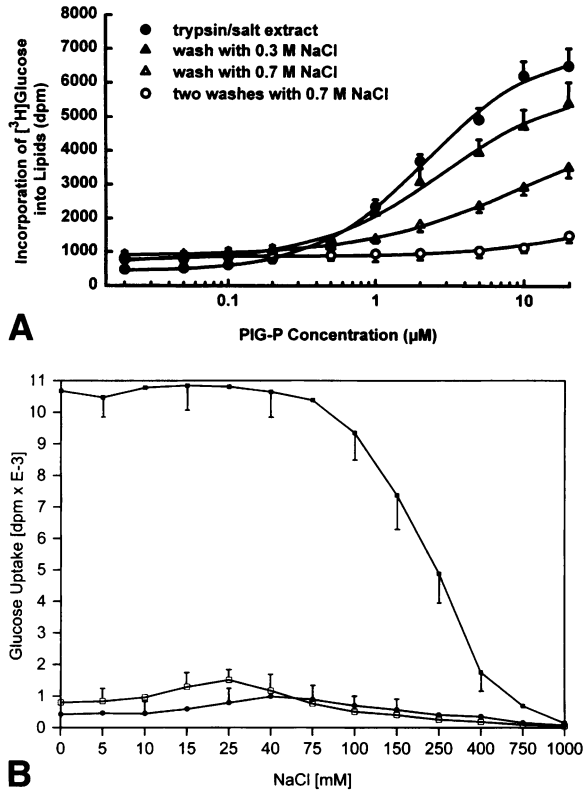

Fig. 9. Effect of salt treatment on the insulin-mimetic activity of PIG-P in reconstituted adipocytes. Isolated rat adipocytes were treated with 100 μg/ml trypsin and subsequently with 0.5 M NaCl, then supplemented with 200 μl of trypsin/salt extract (A and B, open and filled squares) or buffer (B, circles). After reconstitution, the cells were washed three times by flotation as described in the legend to Fig. 8 and then adjusted to 0.3 or 0.7 M NaCl or left without salt (A) or adjusted to increasing concentrations of NaCl (B). Subsequently, the adipocytes were washed twice by flotation (A) or left untreated (B). For one portion of cells, the salt treatment (0.7 M NaCl) was repeated (A). The cells were then assayed for stimulation of lipogenesis (A) or glucose transport (B) in the presence of increasing concentrations of PIG-P (A) or 5 μm PIG-P (B, filled squares) or absence of PIG-P (B, circles and open squares). Each point represents the mean ± SD of four adipocyte preparations and reconstitution reactions, with lipogenesis measurements in triplicate.

above finding, washing of the reconstituted adipocytes with salt immediately after the reconstitution reaction prior to the lipogenesis assay reduced the efficiency of the restoration of both the responsiveness and sensitivity toward PIG-P action in these cells. The degree was dependent on the number and ionic strength of the wash cycles. Apparently, the component required for PIG-P-stimulated lipogenesis is able to reassociate in a functional manner with the adipocyte cell surface through bipolar interactions if the salt concentration during the reconstitution reaction remains under 200 mM.

To exclude the possibility that NaCl remaining in the trypsin/salt extract, despite extensive dialysis, may cause some stimulation of lipogenesis in pretreated or reconstituted adipocytes, cells were incubated with 100 μg/ml trypsin and 0.5 M NaCl, washed, subsequently reconstituted with trypsin/salt extract, and then assayed for basal and PIG-P-stimulated glucose transport in the presence of increasing concentrations of NaCl (Fig. 9B). Treatment of the cells with NaCl caused a maximal 2-fold activation of glucose transport only—between 15 and 40 mM NaCl in reconstituted adipocytes (Fig. 9B, open squares) and between 25 and 75 mM NaCl in pretreated cells (Fig. 9B, circles). This stimulation was far below glucose transport activation provoked by PIG-P in reconstituted adipocytes (Fig. 9B, filled squares). The PIG-P-stimulated glucose transport was impaired in the presence of NaCl during the transport assay in a concentration-dependent fashion, with half-maximal inhibition at 200 mM and significant interference starting at 75 mM (Fig. 9B, filled squares). This may be due to blockade of the reassociation of the putative trypsin/salt–sensitive component with the adipocyte cell surface (see above) in combination with loss of cell viability. Apparently, these amounts of salt were not introduced by the addition of the trypsin/salt extract. In conclusion, limited amounts of NaCl possibly contained in the trypsin/salt extract cannot explain the PIG-P-induced insulin-mimetic activity in reconstituted adipocytes.

Trypsin/Salt Extract Harbors a Binding Protein for PIG-P

We first studied the nature of the component contained in the trypsin/salt extract and that was responsible for the reconstitution. Replacement of trypsin for V8 protease from *S. aureus* for preparation of the extract or treatment of the trypsin/salt extract with heat, proteinase K, or NEM prior to the reconstitution assay generated extracts that were completely inefficient in causing reconstitution of trypsin/salt–treated adipocytes for stimulation of lipogenesis by PIG-P (Fig. 10). These data, together with the nondialyzable character of the reconstitution activity using a membrane of 10 kD exclusion size (Fig. 10), strongly suggest that the component released

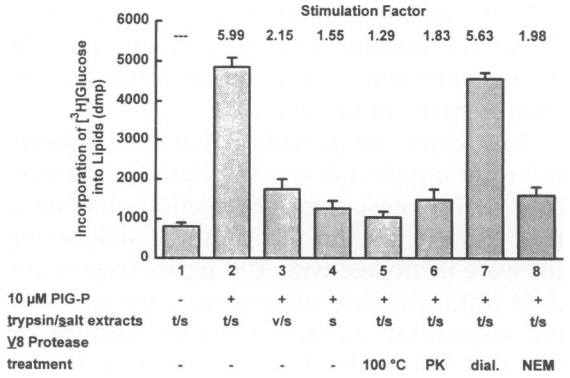

Fig. 10. Inactivation of the trypsin/salt extract for reconstitution of trypsin/salt–treated adipocyte. Isolated rat adipocytes desensitized for PIG-P action by combined trypsin/salt treatment were supplemented with 200 µl of trypsin/salt extract (t/s), which had been pretreated with heat, proteinase K (PK), or NEM, or dialyzed (dial.) or left untreated (see Materials and Methods). Alternatively, extracts were pretreated with V8 protease from *Staphylococcus aureus* in the presence of 0.5 M NaCl (v/s) or with 0.5 M NaCl alone (s). After reconstitution, the cells were washed twice by flotation, incubated in the absence or presence of PIG-P (10 µm) as indicated and then assayed for lipogenesis. Each bar represents the mean ± SEM of three different preparations of the extract and reconstitution reactions, with lipogenesis measurements in quadruplicate. The stimulation factor for lipogenesis in adipocytes reconstituted with untreated trypsin/salt extract in the absence of PIG-P was set at 1.

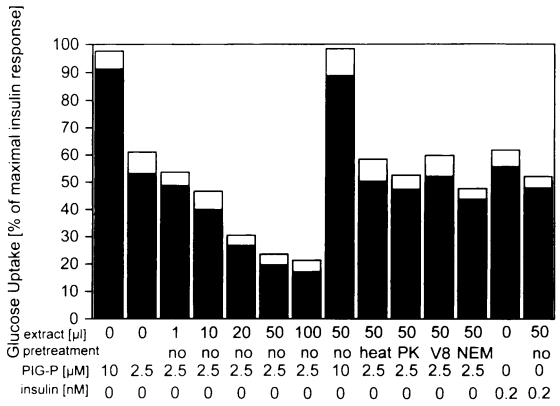

Fig. 11. Effect of the addition of trypsin/salt extract on the stimulation of glucose transport by PIG-P and insulin in untreated adipocytes. Isolated rat adipocytes were incubated (20 min, 37°C) with the indicated volumes of 10-fold concentrated trypsin/salt extract, which had been pretreated with heat, proteinase K (PK), V8 protease (V8), or NEM or had been left untreated (see Materials and Methods), in the absence or presence of the indicated concentrations of PIG-P or insulin and then assayed for glucose transport. Each bar represents the mean (filled portion) ± SEM (open portion) of three different incubations of adipocytes (from three separate preparations) with extract (single preparation), with transport measurements in triplicate. Glucose transport induced by 5 nM insulin was set at 100%.

from the adipocytes by trypsin/salt treatment and required for PIG-P action is a protein or a protein fragment. This proteinaceous component may either directly interact with PIG-P and thus function as receptor protein, or, it may be involved in the transmission of the PIG-P signal from a putative (trypsin- and NEM-insensitive) receptor that is not identical to that component along the cell surface into the interior of the cell.

For differentiation between these possibilities, we tried to inhibit the PIG-P action on untreated adipocytes with an excess of trypsin/salt extract. This would favor the existence of a binding protein in the extract that forms a soluble nonproductive complex with PIG-P, because it fails to associate with the surface of adipocytes not subjected to trypsin/salt treatment. Incubation of untreated adipocytes with trypsin/salt extract reduced the stimulation of glucose transport by 2.5 µm PIG-P in a concentration-dependent fashion (Fig. 11). The approximately 60% maximal inhibition was completely overcome by 10 µm PIG-P, which points to a specific and competitive interaction between PIG-P and the component of the trypsin/salt extract. The detailed study of the glucose transport activation in response to a full range of PIG-P concentrations (0.1–20 µm) in the absence and presence of 50 µl trypsin/salt extract revealed a considerable shift of the concentration–response curve to the right when the extract was present. The EC_{50} value for PIG-P raised from 1.7 ± 0.4 µm (absence of extract) to 5.4 ± 0.9 µm (presence of extract). The sensitivity of the cells toward PIG-P was obviously reduced, whereas the maximal responsiveness (at 20 µm) was not affected by the amount of extract used. Pretreatment of the trypsin/salt extract with heat, proteinase K, V8 protease, or NEM abolished its inhibitory effect on PIG-P-stimulated glucose transport (Fig. 11). This indicates a proteinaceous nature of the inhibitor which may be the component able to reconstitute PIG-P activity in trypsin/salt–treated adipocytes (see below). Interestingly, a concentration of trypsin/salt extract that blocked half-maximal glucose transport activation by PIG-P failed to antagonize half-maximal insulin action (Fig. 11).

Caveolar structures and detergent-insoluble complexes have been attributed a role in insulin-mimetic signaling by PIG structures (see Introduction). Consequently, we investigated whether the trypsin/salt– and NEM-sensitive binding protein required for PIG-P action is a component of detergent-insoluble complexes and caveolae. A trypsin/salt extract was prepared from detergent-insoluble complexes of isolated rat adipocytes using a protocol adapted from the trypsin/salt treatment of intact adipocytes (see Materials and Methods) and then assayed for reconstitution and inhibition of PIG-P activity in trypsin/salt–treated and normal adipocytes, respectively (Fig. 12), as performed for extract isolated from intact adipocytes.

Addition of increasing amounts of trypsin/salt extract prepared from detergent-insoluble complexes to trypsin/salt–treated adipocytes and subsequent reconstitution led to restoration of glucose transport activation by PIG-P (10 μm) to up to 60% of the maximal value obtained with untreated adipocytes (Fig. 12, squares). Conversely, the presence of this extract during incubation of untreated adipocytes with PIG-P (2.5 μm) inhibited in a concentration-dependent manner the glucose transport activation by up to 75% (Fig. 12, circles). Both the inhibition of PIG-P activity in untreated adipocytes as well as the reconstitution of PIG-P activity in pretreated adipocytes was completely abrogated by pretreatment of the trypsin/salt extract from detergent-insoluble complexes with NEM (Fig. 12, asterisks, exes) and V8 protease (data not shown). Extract prepared from detergent-insoluble complexes by treatment with 100 μg/ml trypsin (Fig. 12, diamonds and triangles) or 0.5 M NaCl (data not shown) alone failed to exert activity in both assays. Taken together, these data suggest, but do not prove, that the proteinaceous components required for PIG-P activity that are released into the trypsin/salt extract of intact adipocytes and detergent-insoluble complexes are identical. Furthermore, they raise the possibility that the binding protein for PIG-P is located in certain areas of the adipocyte plasma membrane that correspond to detergent-insoluble complexes.

As a first characterization of the trypsin/salt– and NEM-sensitive component, the polypeptides released by trypsin and/or salt treatment from intact adipocytes were separated by SDS-PAGE (Fig. 13). For visualization of total proteins, the extracts were prepared from intact adipocytes that had been metabolically labeled with

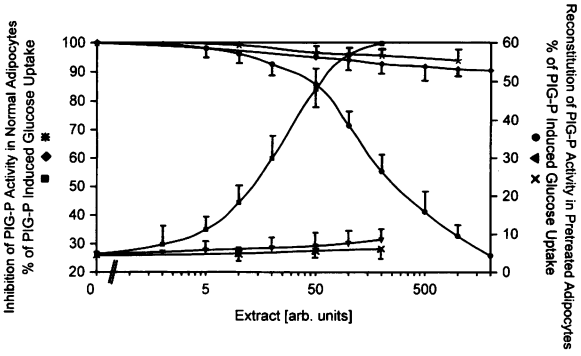

Fig. 12. Effect of the addition of trypsin/salt extract prepared from detergent-insoluble complexes on the stimulation of glucose transport by PIG-P in reconstituted and untreated adipocytes. Isolated rat adipocytes, which had been treated with 100 μg/ml trypsin and 0.5 M NaCl (squares, triangles, exes) or left untreated (circles, diamonds, asterisks) were supplemented with the indicated amounts of normal or 10-fold concentrated trypsin/salt extract (squares, circles) or NEM-treated trypsin/salt extract (triangles, diamonds) or trypsin extract (exes, asterisks), which had been prepared from detergent-insoluble complexes as described in Materials and Methods. The pretreated adipocytes, which had been reconstituted and washed twice by flotation (squares, triangles, exes), as well as the untreated cells (circles, diamonds, asterisks) were incubated with 2.5 μm PIG-P (20 min, 37°C) and subsequently assayed for glucose transport. Each point represents the mean ± SD of four different reconstitutions or incubations using different adipocyte preparations, with extract prepared in triplicate and transport measurements in quadruplicate. The stimulation of glucose uptake was calculated as the difference between the presence and absence of 2.5 μm PIG-P in normal adipocytes and set at 100%, which corresponded to 58 ± 11% of the maximal PIG-P action (at 5 μm) and 43 ± 8% of the maximal insulin action (at 5 nM). Basal glucose uptake in normal adipocytes was set at 0%.

[^{35}S]methionine (Fig. 13, lanes 1–3); for identification of NEM-sensitive proteins, the extracts prepared from unlabeled adipocytes were incubated with [^{14}C]NEM under the same conditions that cause complete inactivation of the trypsin/salt extract by unlabeled NEM (Fig. 13, lanes 4–6). Two [^{35}S]methionine-labeled polypeptides (115 and 49 kD) were identified in the trypsin/salt extract (lane 2) that were not produced by trypsin (lane 1) or salt (lane 3) treatment of the adipocytes alone. The 115-kD protein, but not the 49-kD protein, was radiolabeled upon incubation of the trypsin/salt extract with [^{14}C]NEM (lane 5). Labeling of the 115-kD protein with NEM was completely inhibited in the presence of

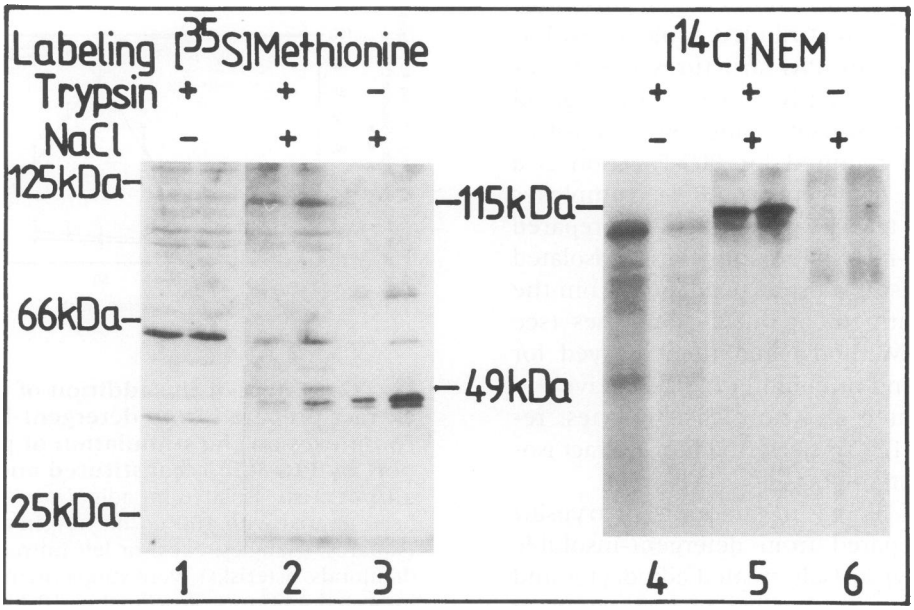

Fig. 13. SDS-PAGE analysis of trypsin-, salt- and NEM-sensitive proteins in adipocytes. Isolated rat adipocytes, which had been metabolically labeled with [^{35}S]methionine (lanes 1–3) or left unlabeled (lanes 4–6), were incubated (20 min, 22°C) with 100 μg/ml trypsin (lanes 1, 2, 4, 5) or left untreated (lanes 3, 6). After termination of the digestion, the cells were adjusted to 0.5 M NaCl (lanes 2, 3, 5, 6) or left untreated (lanes 1, 4) and then separated from the incubation medium by flotation. The infranatant below the cell layer was removed and precipitated with PEG. Equivalent portions (with regard to the number of adipocytes used for the pretreatment) of the [^{35}S]methionine-labeled precipitates were directly dissolved in sample buffer (lanes 1–3), whereas those of the unlabeled precipitates were treated with [^{14}C]NEM (lanes 4–6) as described in Materials and Methods. All samples were analyzed by SDS-PAGE and fluorography. The fluorogram shows the results of two independent extract preparations and labelings with separate adipocyte preparations each. The molecular weights indicated were derived from marker proteins run in parallel on the same gel.

50 mM DTT (data not shown) and was not obtained with the trypsin (lane 4) or salt (lane 6) extracts.

Similar but less complex protein patterns were found when an analogous experiment was performed with trypsin and/or salt extracts from detergent-insoluble complexes of adipocytes (data not shown). Remarkably, a [^{35}S]methionine-labeled 115-kD polypeptide was released from detergent-insoluble complexes of metabolically labeled cells upon trypsin/salt treatment. When this extract was subsequently incubated with [^{14}C]NEM and separated by SDS-PAGE, a single band of 115 kD was found to harbor both the ^{14}C- and ^{35}S-radiolabels.

In further experiments, the conclusions drawn from the competition assay were confirmed; we succeeded in identifying a protein contained in the trypsin/salt extract of intact adipocytes or detergent-insoluble complexes that specifically binds a radiolabeled derivative of PIG-P with K_d values at 0.1 to 1 μm using a filtration assay in combination with PEG precipitation (data not shown). The partially purified binding protein behaved as a transmembrane protein during solubilization experiments. Limited trypsin treatment rendered the protein soluble without loss of its binding capacity. This protein fragment exhibited the intrinsic property for spontaneous reassociation with adipocyte plasma membranes or detergent-insoluble complexes under certain experimental conditions in vitro. Remarkably, the partially purified extract contained a 115-kD polypeptide amenable to modification with [^{14}C]NEM.

PIG-P Induces Tyrosine Phosphorylation of Caveolin

The finding that a protein that apparently binds PIG-Ps and that is required for their insulin-mimetic activity can be recovered with detergent-insoluble complexes of the plasma membrane points to a putative role of these structures in transmembrane signaling by PIG-P. Since in-

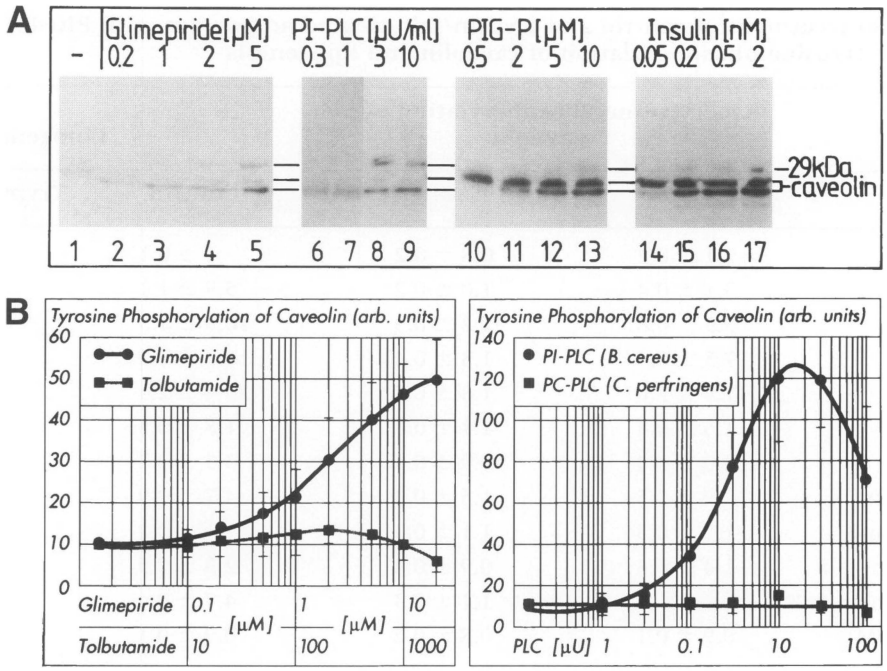

Fig. 14. Effect of treatment of diaphragms and adipocytes with sulfonylureas, PLC, PIG-P, and insulin on tyrosine phosphorylation of caveolin. Isolated rat adipocytes (A) and hemidiaphragms (B) were incubated with increasing concentrations of PI-specific PLC from *Bacillus cereus* or PC-specific PLC from *Chlostridium perfringens* for 40 min at 30°C or glimepiride and tolbutamide for 2 hr at 37°C or PIG-P or insulin for 20 min at 37°C as indicated. Detergent-insoluble complexes were prepared from total fat-free extract of the adipocytes (A) or total membranes of the diaphragms (B), solubilized in TX-100/octylglucoside (as described in Materials and Methods), and subjected to immunoprecipitation with anti-caveolin antibodies under native conditions. The immunoprecipitates were separated by SDS-PAGE and immunoblotted with anti-phosphotyrosine antibodies. Caveolin phosphorylated at tyrosine was detected using [^{125}I]protein A. The quantitative evaluations of the blot (B, each point represents the mean ± SD of four different diaphragm preparations/incubations, with caveolin immunoprecipitations and immunoblots in duplicate) or the autoradiogram (A, representative of three separate experiments for each compound) are shown. The tyrosine-phosphorylated 21- and 24-kD proteins were identified as caveolin by probing of the same blots with anti-caveolin instead of anti-phosphotyrosine antibodies (data not shown). The amounts of caveolin recovered did not differ significantly among the different incubations. The molecular weight of the caveolin-associated 29-kD protein, which did not cross-react with anti-caveolin antibodies in the immunoblot, was derived from marker proteins run in parallel on the same gel.

sulin has been reported to trigger tyrosine phosphorylation of caveolin, a component of detergent-insoluble complexes (see Introduction), we studied the effect of several different agents with insulin-mimetic activity on caveolin phosphorylation. Isolated rat adipocytes (Fig. 14A) and diaphragms (Fig. 14B) were incubated with increasing concentrations of the sulfonylurea drugs glimepiride and tolbutamide for 2 hr, or PI/PC-specific PLC for 40 min, or PIG-P or insulin for 20 min. Detergent-insoluble complexes were prepared from total cell extracts or membranes, respectively, by treatment with 1% TX-100 at 4°C and subsequent sucrose gradient density centrifugation. Caveolin was immunoprecipitated with anti-caveolin antibodies from the detergent-solubilized complexes and assayed for tyrosine phosphorylation by immunoblotting with anti-phosphotyrosine antibodies.

As can be seen from the fluorogram (Fig. 14A, shown for adipocytes only) and the quantitative evaluation of the blot by phosphorimaging analysis (Fig. 14B for diaphragms; Table 1 for adipocytes), the amount of tyrosine-phosphorylated caveolin increased in detergent-insoluble complexes from adipocytes and diaphragms that had been incubated with glimepiride (Fig. 14A, lanes 2–5; Fig. 14B, left section) or PI-specific PLC (Fig. 14A, lanes 6–9; Fig. 14B, right section) in a concentration-de-

Table 1. Effect of treatment of control and trypsin/salt–treated adipocytes with PIG-P, PLC, and sulfonylureas on tyrosine phosphorylation of caveolin and lipogenesis

Assay	Tyrosine Phosphorylation of Caveolin		Lipogenesis	
Cells	Control	Trypsin/salt–treated	Control	Trypsin/salt–treated
Basal	1 ± 0.2	0.8 ± 0.2	1 ± 0.1	1.3 ± 0.1
PIG-P (0.5 μm)	3.1 ± 0.4	1.0 ± 0.2	5.9 ± 1.1	1.5 ± 0.3
PIG-P (2 μm)	5.5 ± 0.8	1.2 ± 0.3	10.9 ± 1.5	1.7 ± 0.3
PIG-P (5 μm)	7.5 ± 0.9	1.3 ± 0.4	16.8 ± 1.9	2.1 ± 0.3
PIG-P (10 μm)	11.9 ± 2.0	1.8 ± 0.5	23.4 ± 2.4	2.5 ± 0.4
PI-PLC (1 μU/ml)	1.6 ± 0.4	1.1 ± 0.3	1.8 ± 0.5	1.2 ± 0.3
PI-PLC (3 μU/ml)	2.0 ± 0.4	0.9 ± 0.1	3.5 ± 0.7	1.3 ± 0.2
PI-PLC (10 μU/ml)	2.9 ± 0.5	1.5 ± 0.3	4.7 ± 0.9	2.0 ± 0.4
PC-PLC (100 μU/ml)	1.2 ± 0.3	1.1 ± 0.3	1.1 ± 0.2	1.4 ± 0.2
Glimepiride (1 μm)	1.4 ± 0.3	0.9 ± 0.4	2.8 ± 0.5	1.1 ± 0.2
Glimepiride (5 μm)	2.4 ± 0.3	1.1 ± 0.3	4.7 ± 0.4	1.5 ± 0.3
Tolbutamide (1 mM)	0.9 ± 0.1	0.8 ± 0.2	0.9 ± 0.1	1.1 ± 0.2

Untreated (control) or trypsin/salt–treated (100 μg/ml trypsin, 0.5 M NaCl) adipocytes (1×10^6 cells/ml) were incubated (37°C) with the indicated concentrations of PIG-P for 20 min or PI/PC-specific PLC for 40 min or glimepiride/tolbutamide for 2 hr. From one portion of cells, detergent-insoluble complexes were prepared and analyzed for tyrosine-phosphorylated caveolin by immunoprecipitation with anti-caveolin antibodies and subsequent immunoblotting with anti-phosphotyrosine antibodies and [^{125}I]protein A (see Materials and Methods). Another portion of cells was assayed for lipogenesis. Each value represents the stimulation factor (above basal) ± SD of three different adipocyte preparations and incubations with caveolin phosphorylation determinations in duplicate and lipogenesis determinations in quadruplicate.

pendent manner to up to 15–25% of the maximal insulin effect. Treatment of isolated rat adipocytes with both glimepiride and PI-specific PLC is known to induce a number of insulin-mimetic actions, such as partial stimulation of glucose transport and lipogenesis (see Table 1; for reviews see refs. 87, 88). The maximal response with glimepiride (obtained at 10 μm) and its EC_{50} value for induction of tyrosine phosphorylation of caveolin recovered with detergent-insoluble complexes in the isolated diaphragm (Fig. 14B) and adipocytes (Fig. 14A, lanes 2–5; Table 1) corresponded well to the concentration–response relationship for the insulin-mimetic activity of this sulfonylurea of the third generation in isolated rat adipocytes (Table 1; see also refs. 87, 88). In contrast, the sulfonylurea of the first generation, tolbutamide, or PC-specific PLC did not cause tyrosine phosphorylation of caveolin to a significant degree in both diaphragms (Fig. 14B) and adipocytes (Fig. 14A; Table 1), despite the use of 100-fold higher concentrations of tolbutamide than of glimepiride. Remarkably, both tolbutamide and PC-specific PLC completely failed to exhibit insulin-mimetic activity in isolated rat adipocytes (Table 1). PIG-P provoked tyrosine phosphorylation of caveolin in a concentration-dependent fashion (Fig. 14A, lanes 10–13), with half-maximal effects at concentrations (1–2 μm) that exhibit insulin-mimetic activity in adipocytes. The maximal increase in tyrosine-phosphorylated caveolin in response to PIG-P (10 μm) approached 80% of the maximal insulin effect (lanes 14–17), which corresponded well to the relative insulin-mimetic potency of PIG-P versus insulin.

Preliminary data indicate that very low concentrations of PIG-P (to up to 0.3 μm) and insulin (to up to 0.05 nM) synergistically increase tyrosine phosphorylation of caveolin in isolated rat adipocytes. In contrast, at concentrations that elicit about 25–50% of maximal caveolin phosphorylation and glucose transport (1–3 μm and 0.1–0.5 nM, respectively), PIG-P and insulin affect caveolin tyrosine phosphorylation in an additive fashion. Further experimentation is required to solve the problem of whether PIG-P and insulin use (in part) the same pathways for triggering tyrosine phosphorylation of caveolin.

In addition to the increments in the 21- and 24-kD forms of phosphorylated caveolin, treatment of adipocytes with glimepiride, PI-PLC, PIG-P, or insulin caused tyrosine phosphorylation of a 29-kD polypeptide in a concentration-dependent fashion (see Fig. 14A). Apparently, this protein is a component of detergent-insoluble complexes and is associated but not identical with caveolin, as it was immunoprecipitated together with caveolin but failed to react with anti-caveolin antibodies in the immunoblot (data not shown). The insulin-induced tyrosine phosphorylation of a 29-kD caveolin-associated protein has been described previously (72), but its nature and function have yet to be established.

Interestingly, induction of tyrosine phosphorylation of caveolin required the functional trypsin/salt–sensitive component. In trypsin/salt–treated adipocytes, the stimulation of both caveolin tyrosine phosphorylation and lipogenesis in response to treatment with PIG-P, PI-specific PLC, and glimepiride was drastically reduced, compared with that in control cells (Table 1). Obviously, lipolytic cleavage of (G)PI structures, spontaneous partitioning of glimepiride molecules into detergent-insoluble complexes, which has been demonstrated recently for isolated rat adipocytes (88), and the action of PIG-P on intact adipocytes share the involvement of the trypsin/salt–sensitive component of the adipocyte plasma membrane for induction of both tyrosine phosphorylation of caveolin and lipogenesis.

Discussion

The results presented here using known inhibitors of insulin action in isolated rat adipocytes and diaphragms suggest that the signaling pathways for PIG-P and insulin are convergent downstream of phosphorylation/activation of IRS-1/PI 3-kinase. Inhibition of PI 3-kinase completely prevented activation of glucose transport and GPAT by PIG-P, whereas blockade of p70S6kinase interfered with PIG-P stimulation of GPAT only. Inhibition of MAPK kinase did not affect PIG-P action on glucose transport and GPAT. The same inhibition pattern in rat adipocytes and diaphragms is true for insulin. The insulin-mimetic activity of PIG-P required a cell surface component that can be released by a combined trypsin/salt treatment from either the membrane of intact adipocytes or detergent-insoluble complexes of adipocyte plasma membranes and manages to reassociate with the membrane in a functional manner. Trypsin/salt–treated adipocytes reconstituted with the trypsin/salt extract regained their sensitivity toward PIG-P. Since the trypsin concentrations used also lead to cleavage of the insulin receptor β-subunit, whose extracellular domain fails to undergo functional reassociation with the adipocyte plasma membrane in a manner analogous to that of the trypsin/salt– and NEM-sensitive component, the experimental protocol of inactivation and reconstitution cannot clarify the involvement of this component in insulin action.

However, excess of trypsin/salt extract added to normal adipocytes competitively inhibited PIG-P action, but not insulin action. The ability of the extract to inhibit or reconstitute the PIG-P activity in untreated and pretreated adipocytes, respectively, was blunted in parallel by several different procedures of pretreatment of the extract. These findings suggest that the NEM-sensitive protein, which restores the insulin-mimetic activity of PIG-P in trypsin/salt–treated adipocytes, functions as binding protein for PIG-P but is not engaged in insulin signaling. This interpretation is compatible with the recent observation that the phosphoprotein patterns generated in isolated rat cardiomyocytes in response to PIG-P and to insulin differ (80), which suggests that there is a partial overlap of the signaling pathways for PIG-P and insulin only. However, at present, we cannot exclude the fact that the peptide moiety of the PIG-P, which may represent an important structural difference to authentic PIG structures, has some influence on the signaling properties. It is conceivable that the tripeptide forms (part of) the epitope recognized by the trypsin/salt– and NEM-sensitive binding protein. Furthermore, insulin may trigger the generation of a structurally (slightly) different PIG(-P) that binds to the trypsin/salt– and NEM-sensitive component with considerably higher affinity than the PIG-P used in the present study. Consequently, the amount of extract used in the competition assay may not have been sufficient to sequester the authentic insulin-sensitive PIG. We are currently addressing the question of whether a peptide-less PIG molecule or structure variants derived from the PIG-P by pronase digestion (see Fig. 1A) also use this component for insulin-mimetic signaling and whether the trypsin/salt extract competes for the activity of these molecules. The answers should shed further light on the relationship of PIG and insulin signaling.

We suggest the following working model for

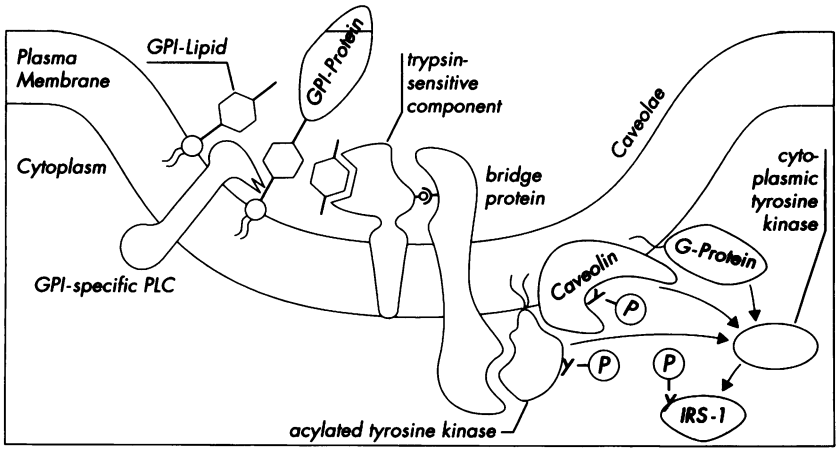

Fig. 15 Hypothetical model for signal transduction from GPI lipids and GPI-anchored proteins across the plasma membrane of insulin-sensitive cells. This signal transduction takes place through the trypsin/salt–and NEM sensitive component, bridge protein and dual acylated tyrosine kinase of the Src-class to tyrosine phosphorylation of signaling proteins, such as IRS-1, caveolin, cytoplasmic (acylated) protein kinases and G proteins. Soluble PIG molecules generated from endogenous GPI structures through cleavage by intrinsic or exogenously added phospholipases or PIG molecules added exogenously cause displacement of endogeneous GPI lipids or GPI membrane protein anchors from their binding site at the trypsin/salt–and NEM-sensitive component located in caveolae. For further details, see Discussion.

signal transduction from a GPI-anchored protein or GPI lipid located at the extracellular face of the plasma membrane across the membrane bilayer by means of acylated tyrosine kinases located at the intracellular face of the membrane to cytoplasmic or microsomal (GLUT4 vesicle–associated) PI 3-kinase. The corresponding signaling components are assumed to have the following topology (Fig. 15): GPI lipids and GPI-anchored proteins interact through certain determinants within their glycan core (and the carboxy-terminal protein portion, respectively) with the trypsin/salt– and NEM-sensitive component, which itself binds through bipolar interactions with an unidentified transmembrane "bridge" protein. This bridge protein is in contact with Src kinases through the fatty acyl chains and certain protein epitopes of the latter. Candidates for the bridge protein may be found within the integrin family. All these components are arranged in a special signaling compartment that may be identical to caveolae and form detergent-insoluble complexes. The model implicates the following mechanism of signal transduction (Fig. 15). Cross-linking of GPI-anchored proteins or GPI lipids (and thus of the trypsin/salt– and NEM-sensitive component) with antibodies (as shown for T cells and neutrophils [51,63]) or with multivalent natural ligands, or dissociation of GPI structures from the trypsin/salt– and NEM-sensitive component either by their lipolytic cleavage (as may occur during treatment of intact cells with PI-specific PLC; see ref. 89 and present study) or by competition with an excess of complete GPI anchors (90) or soluble PIG(-P) molecules (as putatively performed in the present and previous studies; for reviews see refs. 12,13) will result in a conformational change in the trypsin/salt– and NEM-sensitive component that is transmitted through bipolar interactions to the bridge protein. The bridge protein itself transduces the signal across the membrane, thereby activating the associated tyrosine kinase, presumably through induction of a conformational change. The activated and autophosphorylated tyrosine kinase will phosphorylate signaling proteins, such as IRS-1, caveolin, cytoplasmic tyrosine kinases, and G proteins. Tyrosine phosphorylation of IRS-1 may initiate downstream signaling to glucose and lipid metabolism through PI 3-kinase and complex lipid and serine/threonine kinase cascades. Compatible with the "caveolae model" of PIG signaling is our finding that there is no experimental evidence for specific and rapid transport of a ^{14}C-labeled derivative of the PIG-P into the cytosol of isolated rat adipocytes or 3T3-L1 adipocytes (data not shown), which would be a prerequisite for the "mediator model."

The marked and rapid induction of tyrosine

phosphorylation of IRS-1 and of phosphorylation of additional proteins in response to PIG-P (80) raises the question of which kinase(s) are involved. It has now been recognized that tyrosine phosphorylation of IRS-1 is not restricted to receptor tyrosine kinases, but it can also be mediated by the growth hormone receptor as well as certain cytokine and G protein–coupled receptors (91–96). It is speculated that these receptors directly or indirectly couple to the trypsin/salt– and NEM-sensitive component, thereby inducing tyrosine phosphorylation of IRS-1 through activation of the same acylated nonreceptor tyrosine kinase(s) as those used by the PIG-P.

It may be of relevance in this respect that there seems to be a correlation between the ability of PIG-P to induce tyrosine phosphorylation of caveolin as well as of an unidentified 29-kD protein and its capability to exert insulin-mimetic activity in insulin-sensitive cells. This finding supports the involvement of caveolin (phosphorylation) in signal transduction through PIG-P molecules. Tyrosine phosphorylation of caveolin has also been observed after incubation in vitro of detergent-insoluble complexes isolated from insulin-stimulated adipocytes with Mg^{2+}ATP (72). Since insulin receptors could not be detected in these complexes, caveolin must have been phosphorylated by a nonreceptor tyrosine kinase associated with the complexes. One kinase identified was $p59^{fyn}$, a member of the cytoplasmic tyrosine kinases of the Src family (72). Recently, a GPI anchor alone was shown to induce in macrophages a rapid onset of tyrosine phosphorylation of proteins that may be involved in the regulation of the IL-1α and TNF-α expression (90)—among them, polypeptides of the size of caveolin.

The proteinaceous trypsin/salt– and NEM-sensitive component may be embedded in the plasma membrane by means of a transmembrane domain and interact through salt bridges with the transmembrane bridge protein. This interaction, which might guarantee peripheral association of the extracellular PIG-P binding domain of the component with the cell surface upon trypsin cleavage of its membrane anchor, seems to be sufficient for mediating PIG-P action. It may thus form the molecular basis for reconstitution of PIG-P action in trypsin/salt–treated adipocytes upon addition of the trypsin/salt extract. At present, we are trying to identify the bridge protein by examining its putative affinity to the partially purified trypsin/salt– and NEM-sensitive component; this requires performing chemical cross-linking with bifunctional photolabile reagents or co-purification using the competition assay. Furthermore, successful reconstitution of PIG-P signaling in a cell-free system consisting of detergent-insoluble complexes, including the trypsin/salt– and NEM-sensitive component and bridge protein(s) in terms of PIG-P-dependent activation of the associated tyrosine kinase(s) and tyrosine phosphorylation of caveolin, would strongly support our present model for PIG(-P) signaling.

With respect to the putative mechanism of competition of the binding of GPI structures to the trypsin/salt– and NEM-sensitive component, the PIG-P derived from Gce1p of *S. cerevisiae* may be particularly efficient at interacting with this component and thus at displacing authentic GPI structures from their receptor compared with other PIG structures or complete GPI anchors. We have validated this assumption by establishing a preliminary structure–activity relationship for PIG molecules. The most complex PIG-P compounds containing the tripeptide and the complete core glycan, including the mannose side branch according to the GPI anchor of yeast Gce1p and over 50 variants of less complex structure, have been synthesized chemically and studied for insulin-mimetic activity and binding to the trypsin/salt– and NEM-sensitive component in the competition assay. As far as we know, this effort has provided the first synthetic PIG molecules with proven potent insulin-mimetic activity in vitro (W. Frick, A. Bauer, J. Bauer, S. Wied, G. Müller, unpublished results). Preliminary data suggest a strict correlation for weakly active PIG-P derivatives between their ability to stimulate lipogenesis in normal adipocytes and to inhibit PIG-P activation of lipogenesis in the presence of excess of trypsin/salt extract. This strongly argues for involvement of the PIG-P binding protein in insulin-mimetic signaling by PIG-P and for the potency of PIG-P.

Taken together, PIG-P seems to harbor all structural determinants required for insulin signaling independent of the insulin receptor kinase by using a trypsin/salt– and NEM-sensitive component that initiates an alternative signaling cascade for triggering tyrosine phosphorylation of IRS-1 and activation of PI 3-kinase. Thus, PIG-P may manage to regulate cellular glucose and lipid metabolism in an insulin-like fashion in insulin-resistant cells and tissues, which are characterized by reduced insulin-dependent insulin receptor and IRS-1 tyrosine phosphoryla-

tion. This characteristic makes them potentially useful for the treatment of insulin-resistant states, such as metabolic syndrome and type II diabetes (for a review see ref. 97).

Acknowledgments

The authors are grateful to C. Jung, S. Welte, and A. Crecelius for excellent technical assistance (Hoechst Marion Roussel Deutschland GmbH), Prof. J. Eckel for helpful discussions (Institute for Diabetes Research, University of Düsseldorf, Germany), Ms. G. McConaghy (Hoechst Marion Roussel Deutschland GmbH) for expert editorial assistance during preparation of the manuscript, and R. Utermark (Hoechst Marion Roussel Deutschland GmbH) for valuable support in preparing the figures.

References

1. Kahn CR. (1994) Insulin action, diabetogenes, and the cause of type II diabetes. *Diabetes* **43:** 1066–1084.
2. White MF, Kahn CR. (1994) The insulin signaling system. *J. Biol. Chem.* **269:** 1–4.
3. Saltiel AR. (1996) Diverse signaling pathways in the cellular actions of insulin. *Am. J. Physiol.* **270:** 375–385.
4. White MF. (1997) The insulin signalling system and the IRS proteins. *Diabetologia* **40:** S12–S17.
5. Cheatham B, Vlahos CJ, Cheatham L, Wang L, Blenis J, Kahn CR. (1994) Phosphatidylinositol 3-kinase activation is required for insulin stimulation of pp70 S6 kinase, DNA synthesis, and glucose transporter translocation. *Mol. Cell. Biol.* **14:** 4902–4911.
6. Okada T, Kawano Y, Sakakibara T, Hazeki O, Ui M. (1994) Essential role of phosphatidylinositol 3-kinase in insulin-induced glucose transport and antilipolysis in rat adipocytes. *J. Biol. Chem.* **269:** 3568–3573.
7. Liscovitch M, Cantley LC. (1995) Signal transduction and membrane traffic: The PITP/phosphoinositide connection. *Cell* **81:** 659–662.
8. Myers MG, Wang LM, Sun X. (1994) The role of IRS-1/GRB2 complexes in insulin signaling. *Mol. Cell. Biol.* **14:** 3577–3587.
9. Myers MG, White MF. (1995) New frontiers in insulin receptor substrate signaling. *Trends Endocrinol. Metab.* **6:** 209–215.
10. Häring HU. (1991) The insulin receptor: Signalling mechanism and contribution to the pathogenesis of insulin resistance. *Diabetologia* **34:** 848–861.
11. Quon MJ, Butte AJ, Taylor SI. (1994) Insulin signal transduction pathways. *Trends Endocrinol. Metab.* **5:** 369–376.
12. Saltiel AR. (1990) Second messengers of insulin action. *Diabetes Care* **13:** 244–256.
13. Varela-Nieto I, Leon Y, Caro HN. (1996) Cell signalling by inositol phosphoglycans from different species. *Comp. Biochem. Physiol.* **115B:** 223–241.
14. Romero G, Larner J. (1993) Insulin mediators and the mechanism of insulin action. *Adv. Pharmacol.* **24:** 21–50.
15. Jarett L, Kiechle FL, Macaulay SL, Parker JC, Kelly KL. (1985) Intracellular mediators of insulin action. In: Cech MP (ed). *Molecular Basis of Insulin Action*. Plenum Publishing, New York, pp. 171–182.
16. Saltiel AR, Fox JA, Sherline P, Cuatrecasas P. (1986) Insulin stimulates the generation from hepatic plasma membranes of modulators derived from an inositol glycolipid. *Science* **233:** 967–972.
17. Mato JM, Kelly KL, Abler A, Jarett L. (1987) Partial structure of an insulin-sensitive glycophospholipid. *J. Biol. Chem.* **262:** 2131–2137.
18. Mato JM, Kelly KL, Abler A, Jarett L, Corkey BE, Cashel JA, Zopf D. (1987) Partial structure of an insulin-sensitive glycophospholipid. *Biochem. Biophys. Res. Commun.* **146:** 764–770.
19. Low MG, Saltiel AR. (1988) Structural and functional roles of glycosyl-phosphatidylinositol in membranes. *Science* **239:** 268–275.
20. Cross GAM. (1990) Glycolipid anchoring of plasma membrane proteins. *Annu. Rev. Cell Biol.* **6:** 1–39.
21. McConville MJ, Ferguson MAJ. (1993) The structure, biosynthesis and function of glycosylated phosphatidylinositols in the parasitic protozoa and higher eukaryotes. *Biochem. J.* **294:** 305–324.
22. Nosjean O, Briolay A, Roux B. (1997) Mammalian GPI proteins: sorting, membrane residence and functions. *Biochim. Biophys. Acta* **1331:** 153–186.
23. Müller G, Schubert K, Fiedler F, Bandlow W. (1992) The cAMP-binding ectoprotein from *Saccharomyces cerevisiae* is membrane-anchored by glycosyl-phosphatidylinositol. *J. Biol. Chem.* **267:** 25337–25346.
24. Müller G, Wied S, Crecelius A, Kessler A, Eckel J. (1997) Phosphatidylinositolglycan-peptides from yeast potently induce metabolic insulin actions in isolated rat adipocytes, cardiomyocytes, and diaphragms. *Endocrinology* **138:** 3459–3475.
25. Müller G, Dearey E-A, Pünter J. (1993) The sulfonylurea drug, glimepiride, stimulates release of glycosylphosphatidylinositol-anchored plasma membrane proteins from 3T3 adipocytes. *Biochem. J.* **289:** 509–521.
26. Müller G, Dearey E-A, Korndörfer A, Bandlow W. (1994) Stimulation of a glycosyl phosphatidylinositol-specific phospholipase by insulin and the sulfonylurea, glimepiride, in rat adipocytes depends on increased glucose transport. *J. Cell Biol.* **126:** 1267–1276.
27. Müller G, Wetekam E-M, Wied S, Bandlow W. (1994) Membrane association of lipoprotein lipase

and a cAMP-binding ectoprotein in rat adipocytes. *Biochemistry* **33:** 12149–12159.
28. Kahn BB. (1995) Lilly Lecture: Glucose transport: pivotal step in insulin action. *Diabetes* **45:** 1644–1654.
29. Romero GL, Gamez G, Huang LC, Lilley K, Luttrell L. (1990) Anti-inositolglycan antibodies selectively block some of the actions of insulin in intact BC3H1 cells. *Proc. Natl. Acad. Sci. U.S.A.* **87:** 1476–1480.
30. Lazar DF, Knez JJ, Medof ME, Cuatrecasas P, Saltiel AR. (1994) The stimulation of glycogen synthesis by insulin in human erythroleukemia cells requires the synthesis of glycosyl-phosphatidylinositol. *Proc. Natl. Acad. Sci. U.S.A.* **91:** 9665–9669.
31. Fonteles MC, Huang LC, Larner J. (1996) Infusion of pH 2.0 D-chiro-inositol glycan insulin putative mediator normalizes plasma glucose in streptozotocin diabetic rats at a dose equivalent to insulin without inducing hypoglycemia. *Diabetologia* **39:** 731–734.
32. Asplin I, Galasko G, Larner J. (1993) *Chiro*-inositol deficiency and insulin resistance: A comparison of the *chiro*-inositol- and *myo*-inositol-containing insulin mediators isolated from urine, hemodialysate, and muscle of control and type II diabetic subjects. *Proc. Natl. Acad. Sci. U.S.A.* **90:** 5924–5928.
33. Shashkin PN, Shashkina EF, Fernqvist-Forbes E, Zhou Y-P, Grill V, Katz A. (1997) Insulin mediators in man: Effects of glucose ingestion and insulin resistance. *Diabetologia* **40:** 557–563.
34. Saltiel AR, Cuatrecasas P. (1986) Insulin stimulates the generation from hepatic plasma membranes of modulators derived from an inositol glycolipid. *Proc. Natl. Acad. U.S.A.* **83:** 5793–5797.
35. Kelly KL, Merida I, Wong EHA, DiCenzo D, Mato JM. (1987) A phospho-oligosaccharide mimics the effect of insulin to inhibit isoproterenol-dependent phosphorylation of methyltransferase in isolated adipocytes. *J. Biol. Chem.* **262:** 15285–15290.
36. Saltiel AR. (1987) Insulin generates an enzyme modulator from hepatic plasma membranes; regulation of adenosine 3',5'-monophosphate phosphodiesterase, pyruvate dehydrogenase, and adenylate cyclase. *Endocrinology* **120:** 967–972.
37. Saltiel AR, Sorbara-Cazan LR. (1987) Inositol glycan mimics the action of insulin on glucose utilization in rat adipocytes. *Biochem. Biophys. Res. Commun.* **149:** 1084–1092.
38. Vila MC, Milligan G, Standaert ML, Farese RV. (1990) Insulin activates glycerol-3-phosphate acyltransferase (*de novo* phosphatidic acid synthesis) through a phospholipid-derived mediator. Apparent involvement of G_i and activation of a phospholipase C. *Biochemistry* **29:** 8735–8740.
39. Gaulton GN. (1991) Differential regulation of glycosylated phosphatidylinositol subtypes by insulin. *Diabetes* **40:** 1297–1304.
40. Suzuki S, Sugawara K, Satoh Y, Toyota T. (1991) Insulin stimulates the generation of two putative insulin mediators, inositol-glycan and diacylglycerol in BC3H-1 myocytes. *J. Biol. Chem.* **266:** 8115–8121.
41. Misek DE, Saltiel AR. (1992) An inositol phosphate glycan derived from a *Trypanosoma brucei* glycosyl-phosphatidylinositol mimics some of the metabolic actions of insulin. *J. Biol. Chem.* **267:** 16266–16273.
42. Deeg MA, Brass EP, Rosenberry TL. (1993) Inositol glycan phosphate derived from human erythrocyte acetylcholinesterase glycolipid anchor and inositol cyclic 1,2-phosphate antagonize glucagon activation of glycogen phosphorylase. *Diabetes* **42:** 1318–1323.
43. Farese RV, Standaert ML, Yamada K, Huang LC, Zhang C, Cooper DR, Wang Z, Yang Y, Suzuki S, Toyota T, Larner J. (1994) Insulin-induced activation of glycerol-3-phosphate acyltransferase by a *chiro*-inositol-containing insulin mediator is defective in adipocytes of insulin-resistant, type II diabetic, Goto-Kakizaki rats. *Proc. Natl. Acad. Sci. U.S.A.* **91:** 11040–11044.
44. Gaulton GN, Pratt JC. (1994) Glycosylated phosphatidylinositol molecules as second messengers. *Semin. Immunol.* **6:** 97–104.
45. Farese RV. (1990) Lipid-derived mediators in insulin action. *Proc. Soc. Exp. Biol. Med.* **195:** 312–324.
46. Romero GL, Luttrell L, Rogol A, Zeller K, Hewlett E, Larner J. (1988) Phosphatidylinositol-glycan anchors of membrane proteins: Potential precursors of insulin mediators. *Science* **240:** 509–511.
47. Movahedi S, Hooper NM. (1997) Insulin stimulates the release of the glycosyl phosphatidylinositol-anchored membrane dipeptidase from 3T3-L1 adipocytes through the action of a phospholipase C. *Biochem. J.* **326:** 531–537.
48. Larner J. (1987) Banting Lecture: Insulin signaling mechanisms. Lessons from the old testament of glycogen metabolism and the new testament of molecular biology. *Diabetes* **37:** 262–275.
49. Mato JM. (1989) Insulin mediators revisited. *Cell. Signal.* **1:** 143–146.
50. Saltiel AR, Osterman DG, Darnell JC, Sorbara-Cazan LR, Chan BL, Low MG, Cuatrecasas P. (1988) The function of glycosyl phosphoinositides in hormone action. *Phil. Trans. R. Soc. Lond.* **B320:** 345–358.
51. Su B, Waneck GL, Flavell RA, Bothwell ALM. (1991) The glycosyl phosphatidylinositol anchor is critical for Ly-6A/E mediated T cell activation. *J. Cell Biol.* **112:** 377–384.
52. Thomas PM, Samelson LE. (1992) The glycophosphatidylinositol-anchored Thy-1 molecule interacts with the $p60^{fyn}$ protein tyrosine kinase in T cells. *J. Biol. Chem.* **267:** 12317–12322.
53. Anderson RGW. (1993) Caveolae: where incom-

ing and outgoing messengers meet. *Proc. Natl. Acad. Sci. U.S.A.* **90:** 10909–10913.
54. Anderson RGW. (1993) Plasmalemmal caveolae and GPI-anchored membrane proteins. *Curr. Opin. Cell Biol.* **5:** 647–652.
55. Rothberg KG, Henser JE, Donzell WC, Ying Y-S, Glenney JR, Anderson RGW. (1992) Caveolin, a protein component of caveolae membrane coats. *Cell* **68:** 673–682.
56. Kurzchalia TV, Dupree P, Monier S. (1994) VIP21-Caveolin, a protein of the *trans*-golgi network and caveolae. *FEBS Lett.* **346:** 88–91.
57. Ying Y-S, Anderson RGW, Rothberg KG. (1992) Each caveolae contains multiple glycosyl-phosphatidylinositol-anchored membrane proteins. *Cold Spring Harbor Quant. Biol.* **57:** 593–604.
58. Lisanti MP, Scherer PE, Tang ZL, Sargiacomo M. (1994) Caveolae, caveolin and caveolin-rich membrane domains: A signaling hypothesis. *Trends Cell Biol.* **4:** 231–235.
59. Bickel PE, Scherer PE, Schnitzer JE, Oh P, Lisanti MP, Lodish HF. (1997) Flotillin and epidermal surface antigen define a new family of caveolae-associated integral membrane proteins. *J. Biol. Chem.* **272:** 13793–13802.
60. Parton RG. (1996) Caveolae and caveolins. *Curr. Opin. Cell Biol.* **8:** 542–548.
61. Rodgers W, Crise B, Rose JK. (1994) Signals determining protein tyrosine kinase and glycosyl-phosphatidylinositol-anchored protein targeting to a glycolipid-enriched membrane fraction. *Mol. Cell. Biol.* **14:** 5384–5391.
62. Robbins SM, Quintrell NA, Bishop JM. (1995) Myristoylation and differential palmitoylation of the *HCK* protein-tyrosine kinases govern their attachment to membranes and association with caveolae. *Mol. Cell. Biol.* **15:** 3507–3515.
63. Stefanova IV, Horejsi V, Ansotegui IJ, Knapp W, Stockinger H. (1991) GPI-anchored cell-surface molecules complexed to protein tyrosine kinases. *Science* **254:** 1016–1019.
64. Shenoy-Scaria AM, Dietzen DJ, Kwong J, Link DC, Lublin DM. (1994) Cysteine of Src family protein tyrosine kinases determines palmitoylation and localization in caveolae. *J. Cell Biol.* **126:** 353–363.
65. Brown DA. (1993) The tyrosine kinase connection: how GPI-anchored proteins activate T cells. *Curr. Opin. Immunol.* **5:** 349–354.
66. Song KS, Scherer PE, Tang Z, Okamoto T, Li S, Chafel M, Chu C, Kohtz DS, Lisanti MP. (1996) Expression of caveolin-3 in skeletal, cardiac, and smooth muscle cells. *J. Biol. Chem.* **271:** 15160–15165.
67. Scherer PE, Lisanti MP, Baldini G, Sargiacomo M, Mastick CC, Lodish HF. (1994) Induction of caveolin during adipogenesis and association of GLUT4 with caveolin-rich vesicles. *J. Cell Biol.* **127:** 1233–1243.
68. Parpal S, Gustavsson J, Stralfors S. (1995) Isolation of phosphooligosaccharide/phosphoinositol glycan from caveolae and cytosol of insulin-stimulated cells. *J. Cell Biol.* **131:** 125–135.
69. Gustavsson J, Parpal S, Stralfors P. (1996) Insulin-stimulated glucose uptake involves the transition of glucose transporters to a caveolae-rich fraction within the plasma membrane. *Mol. Med.* **2:** 367–372.
70. Kandror KV, Stephens JM, Pilch PF. (1995) Expression and compartmentalization of caveolin in adipose cells: Coordinate regulation with and structural segregation from GLUT4. *J. Cell Biol.* **129:** 999–1006.
71. Munoz P, Mora S, Sevilla L, Kaliman P, Tomas E, Guma A, Testar X, Palacin M, Zorzano A. (1996) Expression and insulin-regulated distribution of caveolin in skeletal muscle. *J. Biol. Chem.* **271:** 8133–8139.
72. Mastick CC, Brady MJ, Saltiel AR. (1995) Insulin stimulates the tyrosine phosphorylation of caveolin. *J. Cell Biol.* **129:** 1523–1531.
73. Müller G, Wied S. (1993) The sulfonylurea drug, glimepiride, stimulates glucose transport, glucose transporter translocation, and dephosphorylation in insulin resistant rat adipocytes *in vitro*. *Diabetes* **42:** 1852–1867.
74. Müller G, Ertl J, Gerl M, Preibisch G. (1997) Leptin impairs metabolic actions of insulin in isolated rat adipocytes. *J. Biol. Chem.* **272:** 10585–10593.
75. Müller G, Wied S, Wetekam E-M, Crecelius A, Unkelbach A, Pünter J. (1994) Stimulation of glucose utilization in 3T3 adipocytes and rat diaphragm in vitro by the sulfonylureas, glimepiride and glibenclamide, is correlated with modulations of the cAMP regulatory cascade. *Biochem. Pharmacol.* **58:** 985–996.
76. Müller G, Jordan H, Petry S, Wetekam E-M, Schindler P. (1997) Analysis of lipid metabolism in adipocytes using a fluorescent fatty acid derivative. I. Insulin stimulation of lipogenesis. *Biochim. Biophys. Acta* **1347:** 23–39.
77. Brown DA, Rose JK. (1992) Sorting of GPI-anchored proteins to glycolipid-enriched membrane subdomains during transport to the apical cell surface. *Cell* **68:** 533–544.
78. Sargiacomo M, Sudol M, Tang Z-L, Lisanti MP. (1993) Signal transducing molecules and glycosyl-phosphatidylinositol-linked proteins from a caveolin-rich insoluble complex in MDCK cells. *J. Cell Biol.* **122:** 789–807.
79. Müller G, Zimmermann R. (1987) Import of honeybee prepromelittin into the endoplasmic reticulum: structural basis for independence of SRP and docking protein. *EMBO J.* **6:** 2099–2107.
80. Kessler A, Müller G, Wied S, Crecelius A, Eckel J. (1998) Signalling pathways of an insulin-mimetic phosphoinositolglycan-peptide in muscle and adipose tissue. *Biochem. J.* **330:** 277–286.
81. Vlahos CJ, Matter WF, Hui KY, Brown RF. (1994) A specific inhibitor of phosphatidylinositol 3-ki-

nase, 2-(4-morpholinyl)-8-phenyl-4H-1-benzopyran-4-one (LY294002). *J. Biol. Chem.* **269:** 5241–5248.
82. Kuo CJ, Chung J, Fiorentino DF, Flanagan WM, Blenis J, Crabree GR. (1992) Rapamycin selectively inhibits interleukin-2 activation of p70 S6 kinase. *Nature* **358:** 70–73.
83. Lazar DF, Wiese RJ, Brady MJ, Mastick CC, Waters SB, Yamauchi K, Pessin JE, Cuatrecasas P, Saltiel AR. (1995) Mitogen-activated protein kinase inhibition does not block the stimulation of glucose utilization by insulin. *J. Biol. Chem.* **270:** 20801–20807.
84. Marte BM, Downward J. (1997) PKB/Akt: connecting phosphoinositide 3-kinase to cell survival and beyond. *Trends Biochem. Sci.* **22:** 355–358.
85. Sekar N, Li J, Shechter Y. (1996) Vanadium salts as insulin substitutes: mechanism of action, scientific and therapeutic tool in diabetes mellitus research. *Crit. Rev. Biochem. Mol. Biol.* **31:** 339–359.
86. Tsiani E, Fantus IG. (1997) Vanadium compounds. Biological actions and potential as pharmacological agents. *Trends Endocrinol. Metab.* **8:** 51–58.
87. Müller G, Satoh Y, Geisen K. (1995) Extrapancreatic effects of sulfonylureas—a comparison between glimepiride and conventional sulfonylureas. *Diabetes Res. Clin. Pract.* **28:** S115–S137.
88. Müller G, Geisen K. (1996) Characterization of the molecular mode of action of the sulfonylurea, glimepiride, at adipocytes. *Horm. Metab. Res.* **28:** 469–487.
89. Macaulay SL, Larkins RG. (1990) Phospholipase C mimics insulin action on pyruvate dehydrogenase and insulin mediator generation but not glucose transport or utilization. *Cell. Signal.* **2:** 9–19.
90. Tachado SD, Schofield L. (1994) Glycosylphosphatidylinositol toxin of *Trypanosoma brucei* regulates IL-1α and TNF-α expression in macrophages by protein tyrosine kinase mediated signal transduction. *Biochem. Biophys. Res. Commun.* **205:** 984–991.
91. Argetsinger LS, Hsu GW, Myers MG, Billestrup N, White MF, Carter-Su C. (1995) Growth hormone, interferon-γ, and leukemia inhibitory factor promoted tyrosyl phosphorylation of insulin receptor substrate-1. *J. Biol. Chem.* **270:** 14685–14692.
92. Johnston JA, Wang L-M, Hanson EP, Sun X-J, White MF, Oakes SA, Pierce JH, O'Shea JJ. (1995) Interleukins 2, 4, 7, and 15 stimulate tyrosine phosphorylation of insulin receptor substrates 1 and 2 in T cells. *J. Biol. Chem.* **270:** 28527–28530.
93. Saad MJA, Velloso LA, Carvalho CRO. (1995) Angiotensin II induces tyrosine phosphorylation of insulin receptor substrate 1 and its association with phosphatidylinositol 3-kinase in rat heart. *Biochem. J.* **310:** 741–744.
94. Uddin S, Yenush L, Sun X-J, Sweet ME, White MF, Platanias LC. (1995) Interferon-α engages the insulin receptor substrate-1 to associate with the phosphatidylinositol 3′-kinase. *J. Biol. Chem.* **270:** 15938–15941.
95. Kowalski-Chauvel A, Pradayrol L, Vaysse N, Seva C. (1996) Gastrin stimulates tyrosine phosphorylation of insulin receptor substrate 1 and its association with Grb2 and the phosphatidylinositol 3-kinase. *J. Biol. Chem.* **271:** 26356–26361.
96. Velloso IA, Folli F, Sun XJ, White MF, Saad MJA, Kahn CR. (1996) Cross-talk between the insulin and angiotensin signaling systems. *Proc. Natl. Acad. Sci. U.S.A.* **93:** 12490–12495.
97. Flier JS. (1993) An overview of insulin resistance. In: Moller DE (ed). *Insulin Resistance*. John Wiley & Sons, New York, pp. 1–7.